4-24-2023

Quantifying Phenotypic Variation Among the Head Photophores and Nasal Rosettes of the Myctophid Species, Diaphus Dumerilii in Relation to Body Size

Ryan E. Byrne
Nova Southeastern University

Thesis of
Ryan E. Byrne

Submitted in Partial Fulfillment of the Requirements for the Degree of

Master of Science
Marine Science

Nova Southeastern University
Halmos College of Arts and Sciences

April 2023

Approved:
Thesis Committee

Committee Chair: Dr. Rosanna Milligan

Committee Member: Dr. Tracey Sutton

Committee Member: Dr. Matthew Johnston

HALMOS COLLEGE OF ARTS AND SCIENCES

QUANTIFYING PHENOTYPIC VARIATION AMONG THE HEAD PHOTOPHORES AND NASAL ROSETTES OF THE MYCTOPHID SPECIES, *DIAPHUS DUMERILII* IN RELATION TO BODY SIZE

Ryan E. Byrne

Submitted to the Faculty of
Halmos College of Arts and Sciences
in partial fulfillment of the requirements for
the degree of Master of Science with a specialty in:

Marine Science

Nova Southeastern University

April 2023

Thesis of
Ryan E. Byrne

Submitted in Partial Fulfillment of the Requirements for the Degree of

Master of Science
Marine Science

Nova Southeastern University
Halmos College of Arts and Sciences

April 2023

Approved:
Thesis Committee

Committee Chair: Dr. Rosanna Milligan

Committee Member: Dr. Tracey Sutton

Committee Member: Dr. Matthew Johnston

Abstract:

The myctophid genus *Diaphus* is known for having highly developed head photophores and nasal rosettes. The head photophores of *Diaphus* are typically enlarged and vary between species and possibly sexes. *Diaphus dumerilii* is also a macrosmatic species with large olfactory organs. The aim of this study is to quantify the variances in location, size, and shape of the head photophores and nasal rosettes between selected individuals from *Diaphus dumerilii* to understand how these variances relate to morphometric measurements such as body length, inferred maturity and nasal rosette size and shape. *Diaphus* possess many highly conserved traits that are useful for species identification, but little is known about the intraspecific characteristics that vary between an individual's sex, size, and maturity. Comparisons were conducted using computer-aided visualization and image analysis tools and multivariate analyses. From these multivariate analyses it was revealed that the head photophore arrangement and nasal rosette size and shape of *Diaphus dumerilii* show significant changes with standard length and inferred maturity. However, the photophore arrangement and nasal rosette size and shape did not show significant differences between sexes. By examining how certain *D. dumerilii* features change with the organism's size and maturity, it is possible to gain more insight into their function and ecology.

Keywords: Photophores, Morphometry, Myctophids, Nasal Rosettes, Gulf of Mexico

Acknowledgements

First, I want to thank my advisor Dr. Rosanna Milligan for the massive amount of help and advice she has given me throughout my time at NSU that has been paramount to the completion of this project. I would also like to thank my committee members Dr. Tracey Sutton and Dr. Matthew Johnston for all their time and input throughout this process. I would like to thank my fellow seascape ecology lab members, past and present, for their willingness to help me even when they had their own projects to work on, as well as for just being fun to hang out in lab with. Finally, thank you to my friends and family who have supported me throughout my time in graduate school.

Table of Contents

List of Figures

List of Tables

Introduction

The deep sea describes the ocean depths below 200 meters and is one of the most biodiverse areas on the planet, encompassing most of the ocean and possessing massive habitat heterogeneity (i.e., has highly variable environmental factors such as seabed, sediment composition, presence of whalefalls, seamounts, etc.; Sutton et al., 2010; Paulus, 2021). As the deep sea is also a historically understudied region (Webb et al., 2010), morphometric studies can bring insight into how deep-sea assemblages such as myctophids may be structured (Caillon et al., 2018; Sutton et al., 2010). The mesopelagic and bathypelagic zones (200-1000 m and 1000-4000 m, respectively) are interesting case studies in fish evolution with large-scale speciation occurring in several families (e.g., Myctophidae and Stomiidae) (Davis et al., 2014; Martinez et al., 2021). Because of the extreme conditions, fishes living in these depths typically require specialized sensory organs, including vision, hearing, electroreception, and pressure tolerance (de Busserolles and Marshall, 2017; Tusset et al., 2018; Sutton and Milligan, 2019). The sensory drive hypothesis puts forth the idea that in all taxa, intraspecific and interspecific communication influences species diversification by prioritizing the development of these sensory systems (Endler, 1992; Boughman, 2002). Bioluminescence is believed to be one sensory characteristic that facilitates speciation in deep-sea fishes (Davis et al., 2014).

Bioluminescence, the emission of light by organisms via chemical reactions, is an incredibly widespread phenomena in the marine environment that is estimated to have evolved at least 40 times among extant marine organisms, suggesting it must be an advantageous attribute that is not difficult to evolve (Haddock et al., 2010). It is believed that bioluminescence plays roles in inter- and intraspecific communication, predator avoidance (e.g., counterillumination), defensive measures (e.g., bioluminescent spray/flash), prey location and prey attraction (Haddock et al., 2010; Widder, 2010). Bioluminescence is typically generated using one of two main methods: luminescence produced by symbiotic bacteria that is incorporated into body tissues or luminescence produced directly by the organism (Haddock et al., 2010). Direct production of bioluminescence by an organism (without symbionts) is most common in fishes and consists of light being emitted via the breakdown of a luciferin (the light emitting molecule) by a luciferase (oxidative enzyme) while oxygen is present (Haddock et al., 2010; Widder, 2010). Many nonsymbiotic luminous organisms only possess the gene for a luciferase and most obtain the luciferin from another source (Haddock et al., 2010). Obtaining the luciferin is

relatively easy for bioluminescent organisms within the water column, as it is found in both luminous and nonluminous prey, so a predator only needs to find a way to develop a luciferase for light production (Haddock et al., 2010; Widder, 2010).

Bioluminescence is present in all species of Myctophidae with only one known exception (*Taaningichthys paurolychnus*; Haddock et al., 2010; Sutton et al., 2020a). There are many different types of luciferins, but myctophids have been proposed to use coelenterazine for bioluminescence (Haddock et al., 2001; Haddock et al., 2010). A recent study by Duchatelet et al. (2019) further supports this hypothesis as the storage forms of coelenterazine were found in the livers, digestive tracts, and other tissues (skin, muscle, stomach, and intestine) of dissected myctophid specimens. Coelenterazine was also found in the gonads of four of the five myctophid specimens dissected, providing evidence towards the maternal transfer of bioluminescent capabilities (Duchatelet et al., 2019). Coelenterazine is utilized by myctophids through the use of light organs called photophores (Haddock et al., 2010; Widder, 2010; Paitio et al., 2020). Myctophids directly control their photophores through the nervous system (Haddock et al., 2010). This direct control allows for highly specialized predator-avoidance and camouflage mechanisms such as counterillumination as well as for communication (Clarke, 1963; Widder, 2010; Paitio et al., 2020). By using ventral photophores to match the downwelling solar light intensity, bioluminescent organisms can conceal their body silhouettes from predators below them (Clark, 1963; Haddock et al., 2010; Paitio et al., 2020). Myctophids possess specialized vision that in order to determine the correct light levels for counterillumination, have evolved several adaptations such as having large eyes, a reflective tapetum lucida, and aphakic gaps to increase eye sensitivity (de Busserolles and Marshall, 2017).

Photophore distribution and size is species-specific and can be sexually dimorphic among myctophids but photophores are generally found on the ventral and lateral body surfaces, as well as on the head and caudal fin (Figure 1; Mesinger and Case, 1990; Haddock et al., 2010; Sutton et al., 2020a). Myctophid photophores are highly modified, having different functions depending on where they are found on the body, with photophores found laterally, ventrally, caudally, and on the head (Mesinger and Case, 1990; Haddock et al., 2010; Widder, 2010). Ventral photophores are typically used to aid in counterillumination while lateral photophores are hypothesized to assist in inter/intraspecies communication (Clark, 1963; Haddock et al., 2010;

Davis et al., 2014). In terms of unique bioluminescent signals, the genus *Diaphus* is noted to exhibit particularly enlarged orbital photophores in many species (Bolin, 1959). Myctophidae, in general, is an incredibly diverse family including 254 species spanning 34 genera (Fricke et al., 2022). *Diaphus* is noted for being the most species rich genus of Myctophidae with 82 species currently described (Fricke et al., 2022). Given that *Diaphus* is an exceptionally diverse genus in an already diverse family, the presence of species-specific orbital light organs may function as a mechanism to further promote species diversity (Davis et al., 2014). Trait-based studies examining ventral and lateral photophores have revealed that species that utilize bioluminescence for communication tend to exhibit higher taxonomic diversity than those that do not (Davis et al., 2014; Claus et al., 2015). Davis et al. (2014), modelled diversification rates in bony fishes based on nuclear and mitochondrial DNA data and the diversification of bioluminescent lineages were analyzed. Myctophidae with lateral species-specific body photophores exhibited exceptional species diversity given the clade age when contrasted against Neoscopelidae (blackchins) and Gonostomatidae (bristlemouths) which only utilize ventral photophores (Davis et al., 2014). Unique bioluminescent signals within a species may aid in speciation, as species recognition could act as a mechanism to promote genetic isolation such has been observed in bioluminescent ostracods (Palumbi, 1994). How the species-specific patterning first arises is unknown, however, there has been evidence pointing towards habitat differences being a mechanism for signaling diversity (Boughman, 2002). When local environments differ, the selection (whether natural or sexual) on signals and perception may be different too (Boughman, 2002).

The photophores on the tail of myctophids are typically large and capable of producing bright flashes of light (Mesinger and Case, 1990). These caudal photophores are believed to highlight the main sexual differences between most Myctophidae genera that possess them, and yet they are absent among *Diaphus* species (Messinger and Case, 1990; Herring, 2007). Instead, the genus *Diaphus* has highly variable forward-facing head photophores (Nafpaktitis, 1968). The luminous dorsonasal (Dn), ventronasal (Vn), antorbital (Ant), and suborbital (So) organs (Figure 1**)** are believed to assist in finding prey via bioluminescence or by inducing fluorescence (Haddock et al., 2010; Battaglia et al., 2014). The hypervariability (i.e., variance in size, shape, and position on the head) among the head luminous organs of *Diaphus* is especially apparent in the ventronasal and suborbital organs as they both can exhibit sexual dimorphism (e.g., in *D.*

mollis, *D. holti,* and *D. meadi*) or may be absent from some species (e.g., absence of So-photophore in *D. dumerilii*) (Herring, 2007; Tusset et al., 2018). The sexual dimorphism of *Diaphus* species usually consists of three head photophores (i.e., Vn, So, Dn) being larger in mature males than in females (Herring, 2007). The antorbital-photophore may also only be present in the males of some species (Herring, 2007). In terms of morphological distinction, the presence or absence of the So photophore has been used to divide *Diaphus* into two morphological groups: Group A (species with So) and Group B (species without So) (Nafpaktitis et al., 1995; Tusset et al., 2018). The overall morphotype of Group A *Diaphus* species appears to follow the general trend of having a relatively deep, short body, and a relatively larger head, eye, and mouth (de Busserolles et al., 2013; Tusset et al., 2018). Group B species are characterized by an enlarged, relatively long body with a relatively smaller head, eye, and mouth (de Busserolles et al., 2013; Tusset et al., 2018). The distinction between Group A and Group B species is so great that some authors have proposed that species without a So-photophore should be grouped within a separate genus (genus *Aethoprora*; Denton, 2014).

Not only limited to visual sensory capabilities, chemoreception and olfaction in the deep sea are widely used as olfactory organs are well developed in a wide spectrum of marine fishes (Jumper and Baird, 1991; Priede, 2017). It is estimated that 80% of bathypelagic fishes exhibit sexual dimorphism in the olfactory systems, with males typically having larger, more complex receptors (Mead, 1964; Marshall, 1967). In a study by Jumper and Baird (1991), it was found that olfaction appears to play a critical role in mate location for hatchetfishes and is most likely viable for mate-finding in other dispersed populations of deep-sea taxa. With the presence of sexually dimorphic olfactory organs in some mesopelagic fishes (e.g., Sternoptychidae), pheromone detection most likely is important in at least some deep-sea taxa (Baird et al., 1990). When testing a hydrodynamic model of pheromone dispersion, Jumper and Baird (1991) found that at 300 m depth, pheromone signals can be detected at a range of 283 meters when continuously emitted. The pheromone detection ranges at this depth largely surpassed the ranges an organism may be able to perceive bioluminescence visually (detection of blue-green bioluminescence reaches a maximum at about 30 m in lanternfish; Baird et al., 1996; Turner et al., 2009). Studies on the olfactory systems of *Diaphus* are extremely limited, however, myctophids are known to be macrosomatic (i.e., possess large olfactory organs in the form of nasal rosettes) indicating that the chemoreception systems of this taxa could be well developed

and may have some use for pheromone detection (Lawry, 1973). Given that pheromone detection largely outranges light detection and is a sexually dimorphic characteristic in most bathypelagic and some mesopelagic fishes, more information is needed in how *Diaphus* olfaction may be using the nasal rosette to assist in species recognition along with the head photophore variability (Marshall, 1967; Jumper and Baird, 1991; Herring, 2000).

While numerous studies have been conducted on the allometric relationships regarding fish length and maturity for example (Roff, 1993; Srijiaya et al., 2010; Véron et al., 2020), very little is understood about how sensory organs such as nasal rosettes and photophores change with fish growth and maturity, especially concerning myctophids. In a study on deep-sea lizardfishes (Synodontidae) by Fishelson et al. (2010), intraspecific differences were found in the dimensions of the nasal rosettes of fish of different standard body-lengths. The dimensions of the nasal rosettes increased with lizardfish growth until adulthood was reached, where the dimensions remained constant (Fishelson et al., 2010). In terms of photophore variations with growth, a study by Clase and Mallefet (2009) noted how the photogenic patterns of velvet belly lantern sharks (*Etmopterus* spinax) changed with ontogeny (sharks varied from 14.0 – 52.5 cm in length). The study found that both the relative surface area covered by luminous zones (aggregations of photophores) and the photophore density of the zones demonstrated growth-linked variations (Claes and Mallefet, 2009). The surfaces areas of most of the zones (rostral, ventral, caudal, and mandibular) showed allometric growth while the photophore densities of all zones scaled negatively (i.e., they decreased with increased growth; Claes and Mallefet, 2009). An ontogenetic increase was found in the heterogeneity of luminous patterns with more mature sharks using the lateral, caudal, and pectoral photophores for intraspecific signaling (Claes and Mallefet, 2009). As nasal rosettes and photophores have been shown to undergo ontogenetic and intraspecific changes in other deep-sea fishes, this study aims to quantify if the same occurs in *Diaphus* species.

Within the Gulf of Mexico (GoM), myctophids are a dominant component of the mesopelagic ecosystem (Gartner et al., 1987). Despite being semi-enclosed, the Gulf of Mexico is considered a part of the general North Atlantic circulation, with the presence of the Loop Current contributing to the biodiversity of the basin by facilitating migrants to move between regions (Gartner et al., 1987; Bangma and Haedrich, 2008; Lindo-Atichati et al., 2012; Bernard

et al., 2022). Milligan and Sutton (2020) found that myctophid community composition appeared to show relatively weak horizontal structuring in the GoM, with high dispersal and limited hard barriers potentially contributing to a lack of discrete assemblages at the 200 km x 700 km area studied. The variable vertical distribution of myctophids with ontogeny may also facilitate such dispersal, as different life stages may prefer different vertical distributions and the speed and direction of water currents vary with depth in the upper 1000 m of the GoM (Jochens and DiMarco, 2008; Milligan and Sutton, 2020). Myctophids spawn small, buoyant eggs and possess non-migratory, epipelagic larvae, both of which are susceptible to dispersal via horizontal advection (Gjøsæter and Tilseth, 1988; Bernhard et al., 2022). Of the myctophid assemblages found in the GoM, the three most abundant *Diaphus* species appear to be *D. dumerilii*, *D. mollis*, and *D. lucidus*, with *D. dumerilii* being one of the three most abundant lanternfish in the whole family (Gartner et al., 1987; Ross et al., 2010; Milligan and Sutton, 2020a). Genetic diversity and connectivity studies between myctophid populations in the GoM have been limited, however, in a recent study by Bernard et al. (2022) it was found that in the three most abundant myctophids of the area (*D. dumerilii, L. guentheri,* and *C. warmingii*), all showed low genetic diversity and high inbreeding despite their large population sizes. In terms of temporal genetic diversity (i.e., changes in diversity between points in time), *D. dumerilii* was the only species that diversity metrics indicated could have at least two genetic clusters (Bernhard et al., 2022). Bernhard et al. (2022) suggests this could be due to potentially rare endemic genotypes in the GoM or may be the result of a rare dispersal event from another genetically diverse source. Considering how speciose myctophids are, and the fact that intraspecific communication is likely contributing to this speciation, low genetic diversity is a surprising find that highlights the need for further studies on the ecology and diversity of myctophids.

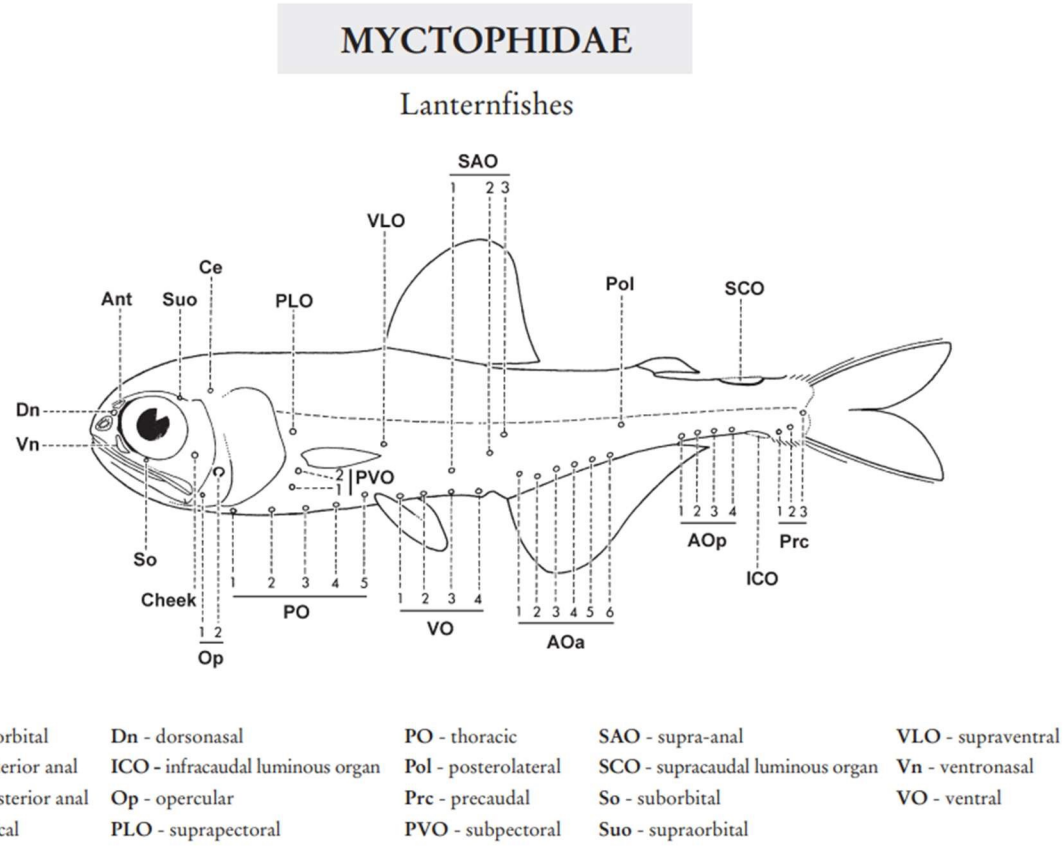

Figure 1 - Distribution and terminology of Myctophidae photophores (adapted from Sutton et al., 2020a)

Study Goals

The primary goal of this study is to quantify shape and positional variations in the head photophores and nasal rosettes of *Diaphus dumerilii* specimens in the Gulf of Mexico, using computer-aided morphometric analyses. I examined how photophore arrangement and relative size changes with body size (as a proxy for maturity) and nasal rosette size within the species and quantify the variance between nasal rosette shapes.

Methodology

Data Collection

For this study, all specimens and metadata were provided by the Deep Pelagic Nekton Dynamics of the Gulf of Mexico consortium (DEEPEND). With the support of the National Oceanic and Atmospheric Administration's (NOAA) Restore Science Program, DEEPEND's objective is to investigate the trends in and drivers of pelagic community structure from the surface to 1500 meters, in the northern Gulf of Mexico. *Diaphus dumerilii* specimens used in this study were collected during the 2022 DP08 cruise aboard the R/V *Point Sur*. Samples were collected during the months of July and August, with the R/V *Point Sur* utilizing a MOCNESS (Multiple Opening Closing Net and Environmental Sensing System) midwater trawl, allowing for discrete-depth sampling of micronekton (Sutton et al., 2020b). The MOCNESS system encompasses six nets that, here, were used to survey specific depth strata from the surface to 1500 meters depth. The majority of the *D. dumerilii* specimens in this study were collected at stations B081 and B082, and from a continental slope station located above Viosca Knoll from depths between 0 and 1000 m. Sample station details are summarized in Table 1. Once sampled, all specimens were identified to the lowest possible taxonomic level and preserved in 4% seawater buffered formalin solution at sea, before being moved to 70% ethanol on land.

Table 1 - Station details including the latitude and longitude, depth range, sample ID, and the number of specimens that were utilized from each station.

Station	Latitude	Longitude	Depth Range	Sample ID	Number of Specimens from Station
B082	27.88623	-87.9884	0-1000	DP08-02AUG22-MOC10-B082N-233-N0-BLK	19
B081	28.4521	-88.0293	0-200	DP08-05AUG22-MOC10-B081N-237-N5	5
Viosca Knoll	29.1248	-88.3828	0-500	DP08-06AUG22-MOC10-UTAHN-239-N5	4

Specimen Selection

The myctophid specimens selected for this study were all stored in Nova Southeastern University's Oceanic Ecology Laboratory. Specimens were selected to encompass a wide size and maturity range of the species (as determined from the literature). The list of the specimens used in this study are shown in Table 2**.**

Maturity Levels

Individuals were divided into four different groups based on maturity and sex: juvenile (15-27 mm), maturing (27-47 mm), mature males (47+ mm and presence of enlarged luminous patch) and females (47+ mm with small luminous patch; Hulley, 1986; Gartner, 1993). Mature males were identified via the enlarged luminous patch present between the dorsonasal photophore and eye, which acts as a mark of sexual dimorphism (Gartner, 1993). Females were identified by specimens with smaller luminous patches that were above the length that male *D. dumerilii* have been known to reach maturity (Hulley, 1986; Gartner et al., 1993). However, Gartner (1993) reported that females of this species do not fully mature until 52 mm SL, so these specimens have been classified as female but not necessarily fully mature. Hulley (1986) reported males reaching maturity at 47 mm SL, which is why they are classified as mature in this study above that length. The maturing group comes from a study by Gartner (1993), in which he found that maturing individuals of *D. dumerilii* were most abundant at 27 mm SL and larger sizes.

Table 2 - *Diaphus dumerilii* specimens used in this study. Standard length, head length, and rosette diameter are all in millimeters (mm). The station refers to where the specimens were collected during the DP08 cruise.

ID	Standard Length	Head Length	Rosette Diameter	Station
Ddum01	22.7	4.9	0.40	B082
Ddum02	28.1	7.2	0.52	B082
Ddum03	22.8	5.2	0.41	B082
Ddum04	31.9	6.5	0.68	B082
Ddum05	17.5	4.0	0.32	B082
Ddum06	28.3	6.1	0.60	B082
Ddum07	29.0	6.8	0.59	B082
Ddum08	17.6	3.7	N/A	B082
Ddum09	25.0	5.4	0.56	B082
Ddum10	29.1	6.9	0.49	B082
Ddum11	26.9	5.7	0.52	B082
Ddum12	19.2	3.8	0.36	B082
Ddum13	29.7	6.5	0.49	B082
Ddum14	18.4	4.0	0.37	B082
Ddum15	28.8	6.6	0.56	B082
Ddum16	17.3	3.7	0.51	B082
Ddum17	44.5	8.8	0.70	B082
Ddum18	41.9	9.0	0.72	B082
Ddum19	16.1	3.5	N/A	B082
Ddum20	46.4	10.0	0.78	B081
Ddum21	40.0	8.8	0.68	B081
Ddum22	26.0	6.2	N/A	B081
Ddum24	42.6	9.1	0.79	B081
Ddum25	31.0	6.5	0.51	B081
Ddum26	34.0	7.1	0.65	Viosca Knoll
Ddum27	48.6	10.2	0.75	Viosca Knoll
Ddum28	56.4	13.1	0.96	Viosca Knoll
Ddum29	47.9	10.6	0.85	Viosca Knoll

Imaging

The myctophid specimens were individually placed on a clear tray filled with ethanol, and oriented to face left over a grey background and a ruler was set under the specimen for scaling. The specimens were viewed and photographed using a microscope camera (Stemi 2000-C microscope with an Axiocam 208 color camera). The microscope zoom was kept constant for all specimens, staying at 9x magnification throughout to ensure that the focus remained the same for all images. The specimens were all illuminated using the built-in lights attached to the microscope. For all images, the region between the tip of the snout to the bottom edge of the operculum where the head ends were the focus (Figure 2). The specimens were all placed with the head as flat against the tray as possible. Every specimen was imaged twice to minimize imaging and human error (Savriama, 2018). Once imaged, all specimens were individually bagged separately from the other trawl fish and given unique ID codes in case further analysis would be needed later. The IDs were based off the genus and species of the specimen (e.g., Ddum01 = the first *Diaphus dumerilii* specimen).

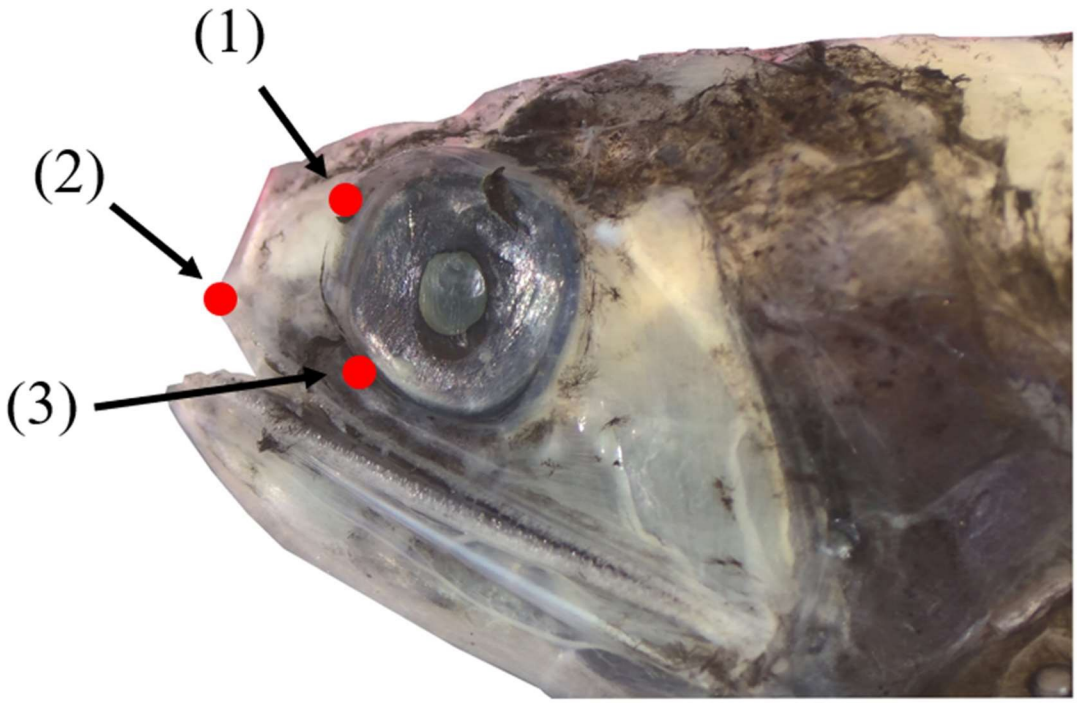

Figure 2 - Specimen Ddum25 highlighting the orientation and focus of the images for landmarking. The nasal rosette, ventronasal (1) and dorsonasal (3) photophore, and tip of upper jaw (2) are all visible.

After each specimen was imaged, the standard length and head length was measured to the nearest millimeter using calipers. The nasal rosette diameters (RD) were measured in tpsDig2 v. 2.31 (Rolhf, 2015) using the ruler from each image as a reference scale. Specimens with damaged or degraded nasal rosettes were excluded from the measurements.

Landmark Analysis

Landmark configuration analysis allows for the digital placement of landmarks along biological structures (Park et al., 2013). By utilizing geometric morphometrics like landmark configurations, patterns and differences between structures can be more accurately discerned than from direct observations (Park et al., 2013). The distance and deformation between landmarks are quantified from one point to another using a coordinate system, or matrix (Cadrin and Friedland., 1999). The deformations in landmark coordinates allow for the use of conventional multivariate analyses (e.g., principal component analysis, discriminant analysis, and cluster analyses; Cadrin and Friedland, 1999). Here, images were loaded into the morphometric software tpsUtil v.1.82 (Rohlf, 2015) for conversion into a TPS file. tpsUtil is a program that allows for the generation of an empty TPS file from a directory of images (Rohlf, 2015). TPS image files are essentially a list of all the specimens containing landmark coordinate data, that can be uploaded into other morphometric software such as tpsDig2 and MorphoJ (Rohlf, 2010a; Klingenberg, 2011). Once the images were combined into a single TPS file, that file was uploaded into tpsDig2 v.2.31 (Rohlf, 2015). tpsDig is a program for digitizing landmarks for morphometric analyses (Rohlf, 2015). Before landmarking could begin, each image, including the duplicates, had to be properly labeled with an identifier within tpsDig and the scale set using the ruler placed under the specimens combined with the measure tool in tpsDig. Once completed, landmarks were manually placed on the head photophores (ventronasal and dorsonasal) as well as the tip of the upper jaw (Figure 2). The jaw landmark was chosen to act as an "anchor point" against which the two photophore landmarks could be compared. For landmarks involving the dorsonasal photophore, the landmark was always placed on the most ventral point to account for potential variations in shape. Once all images were landmarked, the coordinate data were saved to the TPS file and exported to MorphoJ.

MorphoJ is software designed to analyze two- and three-dimensional landmark data through the use of multivariate analyses (Klingenberg, 2011). In order to extract shape information from the images, a Procrustes superimposition aligned by principal axes was performed. The Procrustes superimposition removes the absolute size, position, and rotation of an object to produce a new set of relativized shape variables for further analysis (Gower, 1975). No outliers were found in the dataset of landmark points. A wireframe was generated from the landmarks chosen in this study so that it could act as a visual representation of the overall shape of the landmarks and was created by manually linking all landmarked points within MorphoJ. With the Procrustes fit and wireframe set up, multivariate analyses could be conducted on the Procrustes coordinates.

Outline Analysis

To begin the outline analysis, the images of the specimens were first exported to the open-source image editing software GIMP (GNU Image Manipulation Program; GIMP Development Team, 2022). As the nasal rosettes were the focus of the outline analysis, they had to be isolated from the rest of the image. The Paths Tool was utilized to manually create an outline that was filled in with black to create the "silhouette" (Figure 3). The silhouettes of the nasal rosettes were then exported as jpegs into their own locations. Seventeen nasal rosette silhouettes were created and exported into R Studio.

Figure 3 - Specimen Ddum029 with the nasal rosette visible. An upscaled silhouette of the rosette is overlain to the left of the image.

Once the outlines were created, they were imported into the R package Momocs (Modern Morphometrics; Bonhomme et al., 2014; R Development Core Team, 2023). Momocs is a shape analysis package that can extract quantitative variables from shape information (Bonhomme et al., 2014). Outline analysis differs from landmark analysis in that where landmark analysis examines the relative positioning of landmarks as coordinates, outline analysis estimates scalar descriptors, using various functions to describe aspects of the overall shape (e.g., area, rectangularity, circularity, caliper size, etc.; Bonhomme et al., 2014). All manually created outlines were uploaded into Momocs and used to create coordinate outline matrices (coo). Coos are extracted outlines that Momocs uses to generate scalars from. Once the coo was created, the outlines were aligned using the panel function to visually assess and confirm the shapes were imported correctly. The coo_scalar function was then utilized to generate 15 scalar descriptors for every outline and tested for collinearity. If pairs of scalars were identified as strongly correlated, one of the pair was excluded. In total, the 15 scalars used to describe the outlines of the rosettes were: area, caliper length, centroid size, circularity, Haralick circularity, normalized circularity, convexity, eccentricity bounding box (aspect ratio), eccentricity eigenvalue, elongation, length, width, perimeter, rectangularity, and solidity. Of the fifteen scalars included

in the Momocs package, five were cut to reduce redundancy (normalized circularity, eccentricity eigenvalues, perimeter, length, and width). Normalized circularity was excluded because the data were already normalized within PRIMER. Eccentricity eigenvalue was excluded because the eccentricity value was already being calculated using eccentricity bounding box. Perimeter and width were excluded due to the very high correlation between both variables and area (correlation coefficient = 0.982 and 0.979, respectively). Length was removed due to the high correlation with caliper length (correlation coefficient = 0.997). The remaining ten scalars are described in Table 3. Once chosen, the scalars were imported into PRIMER v7 (Clarke and Gorley, 2015) for further multivariate analyses.

Table 3 - The scalar descriptors, including equations and overall descriptions, used in this study. All scalars are described by Rosin (2005).

Scalar Descriptors	Equation	Meaning
Area	No. of pixels	The total number of pixels in the object.
Caliper Length	$\preccurlyeq F \succ= \frac{P}{\pi}$	Ratio of the perimeter (P) and pi. Describes the longest distance between two points of the object.
Centroid Size	$\sqrt{\sum \quad \lvert p - t \rvert}$	Square root of the sum of squared distances of all the points of an object from the central point.
Circularity	$\frac{P}{area}$	Also called compactness, circularity is how close the object resembles a circle and is calculated using the squared perimeter divided by the area.
Haralick Circularity	$\frac{\mu R}{\sigma R}$	Alternative to tradition circularity, Haralick circularity describes the distance (R) between the center and any point of the perimeter of the object.
Convexity	$\frac{area(X)}{area(CH(X))}$	Ratio of the area (X) and the area of the convex hull of the same region X. Describes how the object differs from a convex shape.
Eccentricity Bounding Box	$EBB = \frac{L}{W}$	Ratio of maximum distance L from the maximum distance W that is perpendicular to L. Describes the length vs width ratio.
Elongation	$EL = \frac{area(X)}{area(MBR)}$	Ratio between the length and width of the objects bounding box. Describes the overall elongation of the object.
Rectangularity	$\frac{area(X)}{area(MBR)}$	Ratio of the area of a region (X) and the area of its minimum bounding rectangle (MBR). Describes how close an object resembles a rectangle.
Solidity	$\frac{\boldsymbol{area}}{\boldsymbol{convex\ area}}$	Ratio of the total area of the object and the area of the convex hull that encloses the object. Describes density of an object.

Statistical Analyses

Morphometric Measurements

Traditional morphometric measurements of the specimens were analyzed. The lengths were all tested for normality using a Shapiro-Wilks test, with the standard length requiring a log transformation to correct skew. Once normalized, a Pearson correlation test was run on all three variables (SL, HL, and RD) against each other. A simple regression was also run between all variables within R Studio to represent the correlation graphically.

Landmark Analyses

For the landmark analyses, the potential measurement error was tested using a one-way Procrustes ANOVA (Savriama, 2018). The Procrustes ANOVA compared the means of the duplicate images to the means of the individual variations to compare the magnitude of variation between individual fish compared to the variation between the duplicate images of the same individual. The results quantify the digitization error of manually placing the landmarks.

Within MorphoJ, a covariance matrix was created for the landmarked points. Next, a Principal Component Analysis (PCA) was run on the Procrustes fitted data. A PCA is an exploratory data analysis tool used to reduce the dimensionality of a dataset while preserving as much original variation as possible (Jolliffe and Cadima, 2016). To test for ontogenetic changes in photophore arrangement, a multivariate regression was run on the Procrustes coordinates against the log-transformed standard length (Foth et al., 2013). Regressions were also run on the first two PC axes versus the log-transformed standard length. For there to be evidence of ontogenetic differences, a significant correlation would need to be present between size and shape on the photophore positions. To further test for a correlation between size and shape, a two-block partial least squares (2B-PLS) was run in MorphoJ on the Procrustes coordinates and standard length. 2B-PLS is a method that compares the covariation between two sets of variables by creating pairs of variables made up of linear combinations of the variables within each data set, essentially being a multivariate correlation test (Foth et al., 2013). Both these methods were also run to test for allometric relationships between the variables (HL and RD) and photophore arrangement.

The landmark data (TPS file) were imported into PRIMER v7 (Clarke and Gorley, 2015), then the data were normalized and additional normalized PCA analyses could be run. With the data in PRIMER, the overall resemblance of the photophore arrangement was analyzed using Euclidean distance for further analyses. Once similarity coefficients were generated, one-way analyses of similarities (ANOSIM) tests were performed (with 10000 permutations) to test for differences between the unordered maturity class groups.

Outline Analyses

Pairwise linear regressions were run between all ten selected scalars and the standard length of the specimens in R Studio (R Core Development Team, 2023) to test for potential shape variation with standard length.

In PRIMER v7 (Clarke and Gorley, 2015), the scalars were first normalized, and then principal component analyses were run on both the nasal rosette and photophore descriptors. Similar to the landmark data, the overall resemblance of the shape descriptors was analyzed via Euclidean distance and ANOSIM tests were performed. A hierarchical cluster analysis (with SIMPROF) was also performed. The cluster analysis was based on the group average and the SIMPROF was a type 1 SIMPROF with 999 permutations.

Results

Traditional Morphometrics

When testing the correlation between the SL, HL, and RD, all three variables showed significant correlations with each other ($p < 0.05$; Figure 4)

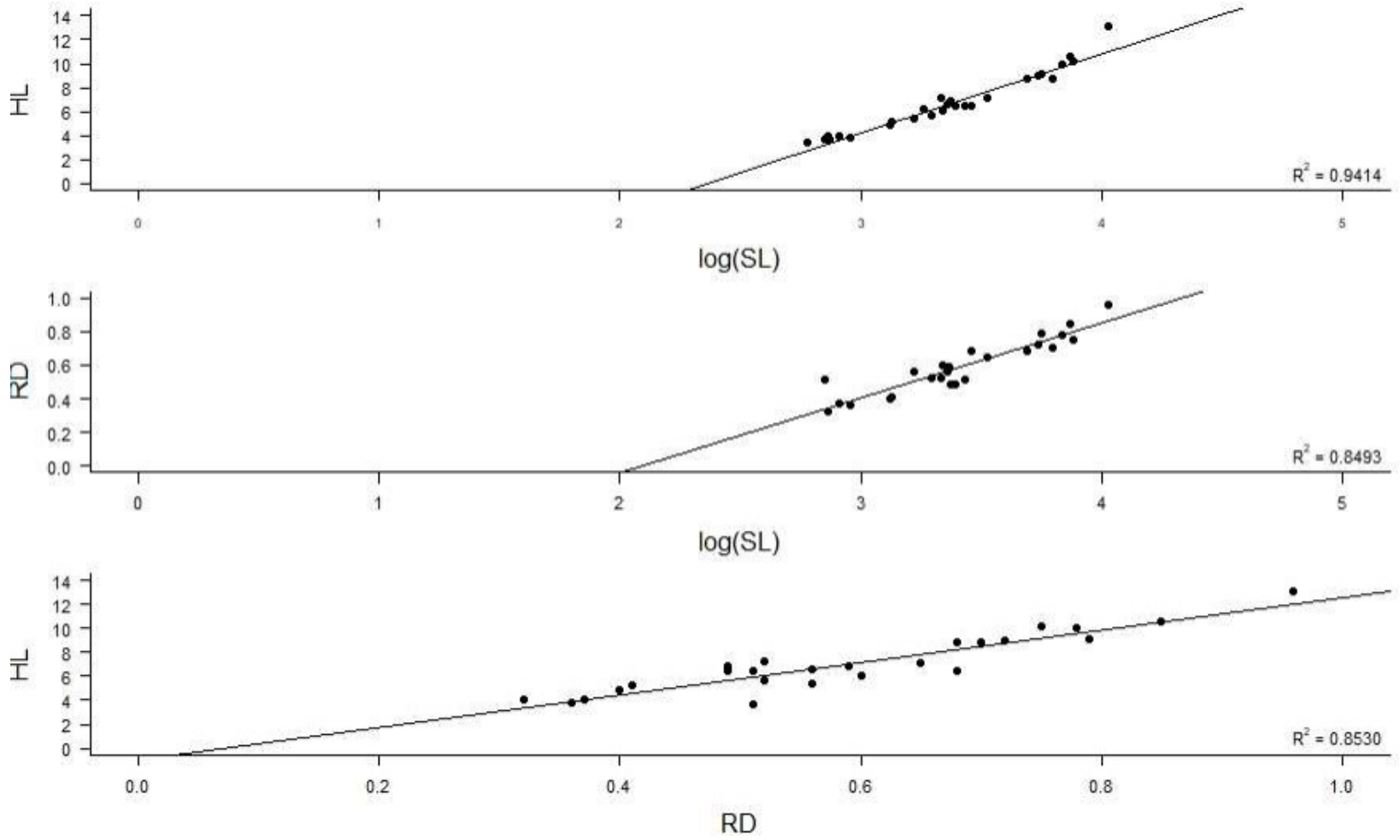

Figure 4 - Linear regressions of the SL, HL, and RD with R-squared. All three measurements were significantly associated with each other.

Landmark Analysis

Imaging/Digitization Error

The Procrustes ANOVA revealed that the size and shape variation among individuals was significant ($p<0.001$), meaning the individual variation among specimens was greater than potential digitization errors when placing the landmarks. The ratio of the F-values indicates that the landmark variation between individual fishes is between 140 and 605 times larger than the variation between the two duplicates of each of the images taken (Table 4), indicating the photophore arrangement between individuals had a much larger impact on the results than the arrangement between the duplicates.

Table 4 - Procrustes ANOVA results for potential digitization error on the Procrustes coordinates between each individual specimen versus the coordinates of the duplicates, where SS = sum of squares, MS = mean squares, df = degrees of freedom, F = F-value and P = p-value.

Procrustes ANOVA					
Effect:	**SS**	**MS**	**df**	**F**	**P**
Individual	13.646	0.5054	27	605.95	<0.0001
Digitization	0.0233	0.0008	28		
Centroid Size ANOVA:					
Individual	0.9119	0.01688	54	140.70	<0.0001
Digitization	0.0067	0.00012	56		

Shape and Size Variation

A PCA of the landmark coordinates showed that PCs 1 and 2 describe 100% of the cumulative variance in photophore arrangement (PC1 = 54.8%, PC2 = 45.2%; Figure 5, Table 5).

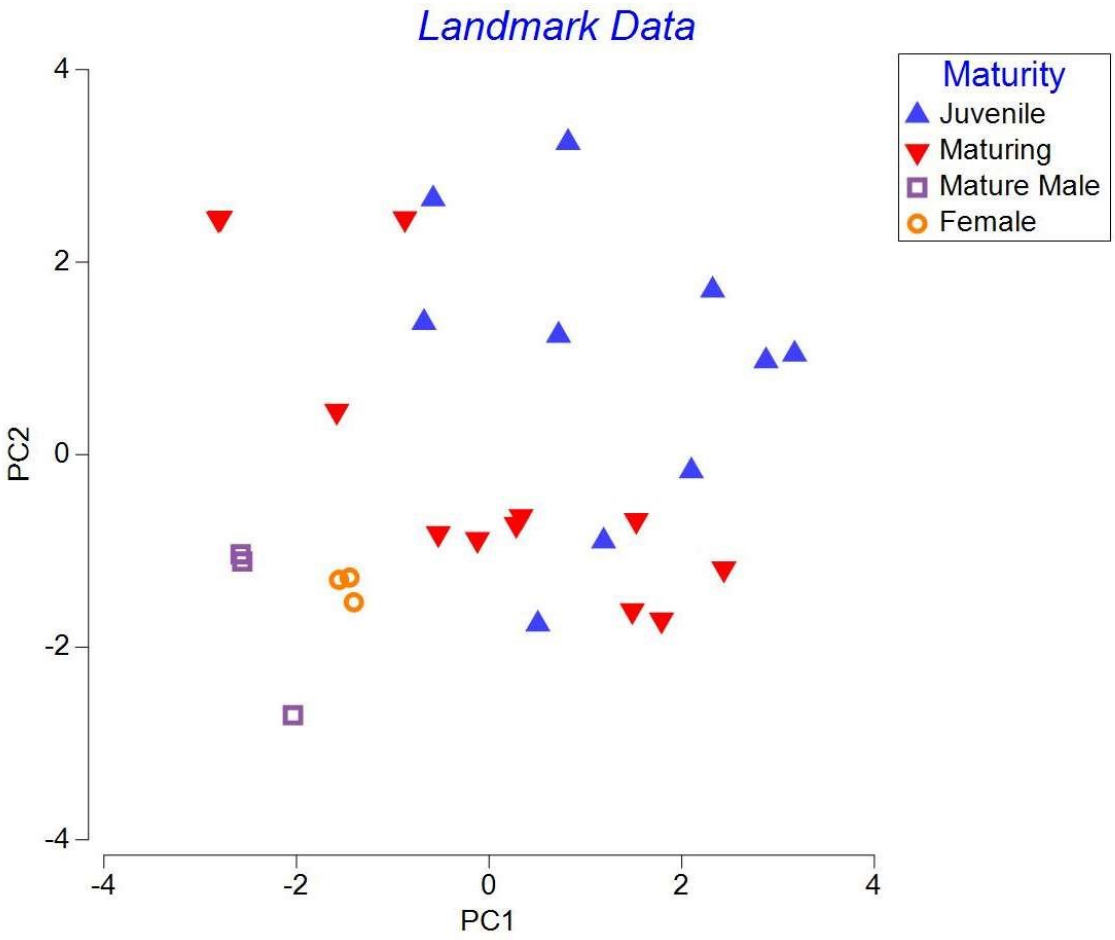

Figure 5 - Normalized PCA of photophore arrangement and size class. The X-coordinates of the three landmarked points are represented by X1, X2, and X3. The Y-coordinates of the three landmarked points are represented by Y1, Y2, and Y3. Maturity levels are represented by different colors and shapes (Juvenile = blue triangle, Maturing = red upside-down triangle, Mature Male = purple square, and Female = orange circle. PC1 explains 54.8% of the variation and PC2 explains 45.2% of the variation.

Table 5 - Absolute values from the PC1 and PC2 on the Procrustes coordinate landmarks. The values represent the overall contribution to the shape variation in each PC, with a higher absolute value indicating a greater contribution.

Landmark	PC1	PC2
X1	0.324	0.491
Y1	-0.506	0.243
X2	-0.529	-0.126
Y2	0.134	-0.589
X3	0.255	-0.538
Y3	0.515	0.216

After the PCA was conducted on the landmarked points, a wireframe graph depicting the overall shape changes of the photophore arrangement was generated (Figure 5). A visual assessment of the wireframe indicates that for PC1, Landmark 1 (Dn photophore) displayed the most variation, followed by Landmark 3 (Vn photophore), and then Landmark 2 (tip of upper jaw). The same order of shape variation appears to be present in PC 2. In both PCs, LMs 2 and 3 show very similar shape changes, with LM 1 always displaying the most variation. A full display of the landmarked points and the variance around them is shown in Figure 6.

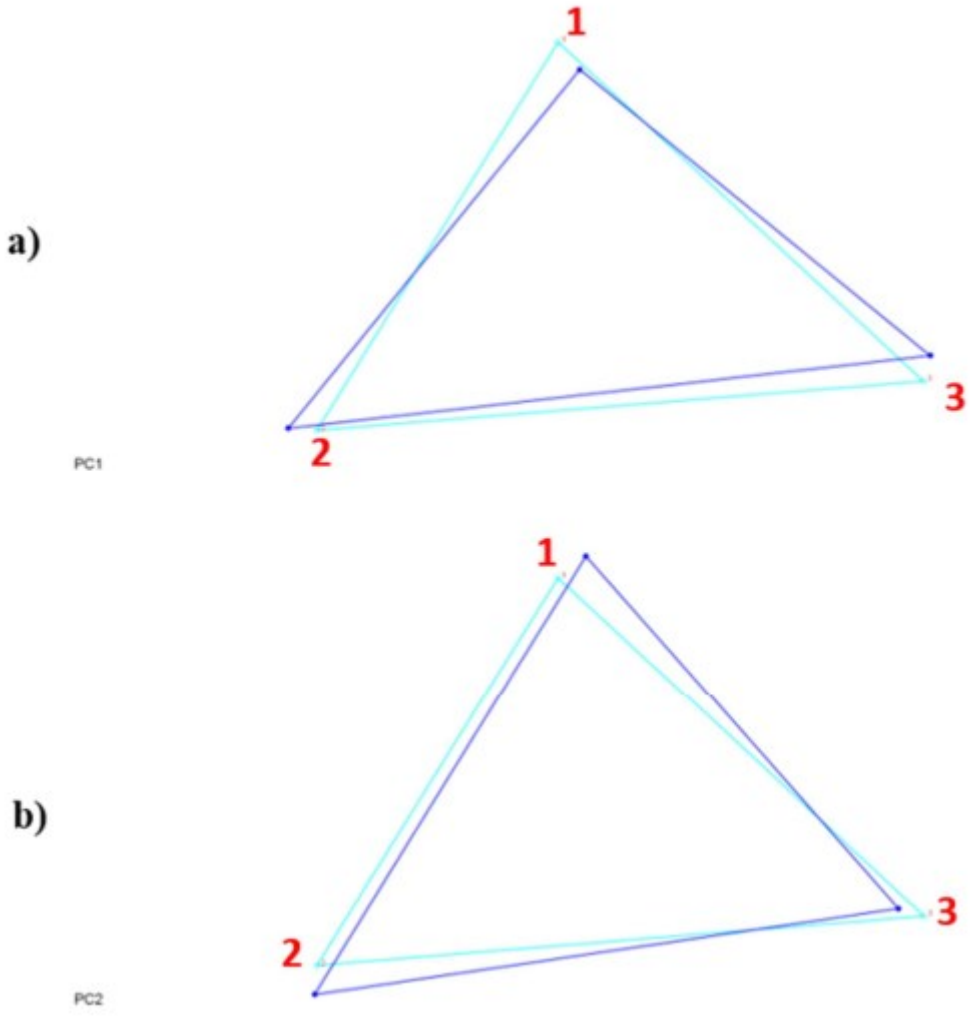

Figure 6 - Results of the wireframe figures representing the shape of the landmarked points. The dark blue lines represent the mean outline configuration while the light blue outlines represent the shape variation. a) Variation of PC1. b) Variation of PC2.

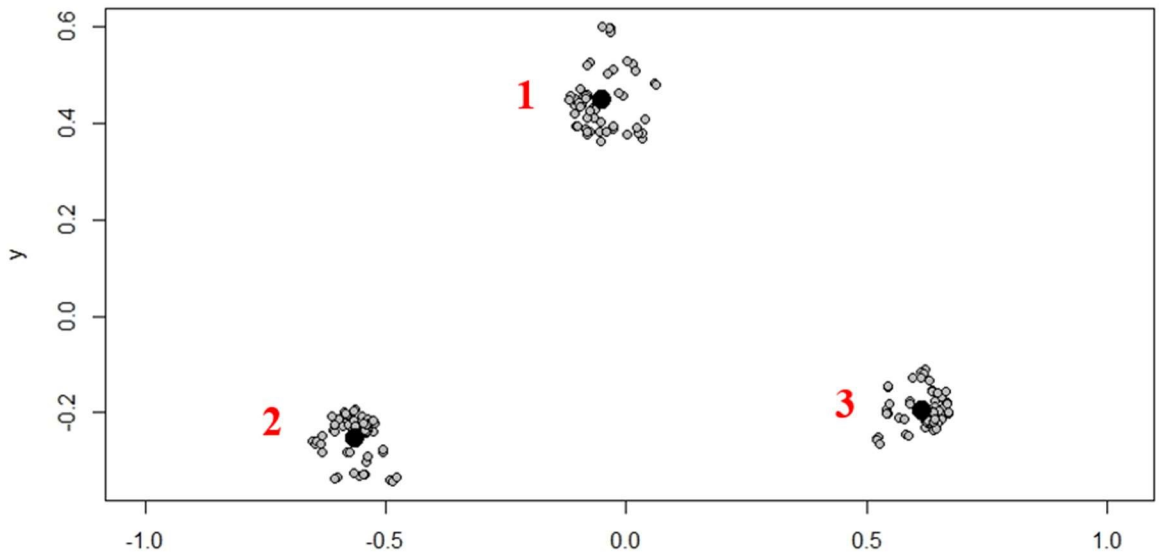

Figure 7 - Means of the three landmarked points of all specimens after the Procrustes superimposition was performed. The black dots represent the mean locations of the three landmarked points, while the grey dots represent all the landmarked points of all specimens.

One-way ANOSIM analysis showed a significant association between the photophore arrangement and the presumed maturity of the specimens (Global R Statistic = 0.268, p-value = 0.004). The pairwise tests showed there was a significant difference between juveniles and maturing specimens (R Statistic = 0.142, p-value = 0.049), juveniles and females (R Statistic = 0.647, p-value = 0.001), and juveniles and mature males (R Statistic = 0.813, p-value = 0.015; Table 6). There was not a significant difference between the maturing specimens and females (R Statistic = 0.126, p-value = 0.172), maturing specimens and mature males (R Statistic = 0.327, p-value = 0.088), and females and mature males (R Statistic = 0.321, p-value = 0.267; Table 6).

Table 6 - Pairwise test results from the ANOSIM run on the maturity levels of the specimens based on the landmarked points. Significant p-values (<0.05) are in bold.

Groups	R Statistic	P-values	Possible Permutations	Actual Permutations
Juvenile, Maturing	0.142	**0.049**	646646	999
Juvenile, Female	0.647	**0.001**	1001	999
Juvenile, Mature Male	0.813	**0.015**	66	66
Maturing, Female	0.126	0.172	1820	999
Maturing, Mature Male	0.327	0.088	999	171
Female, Mature Male	0.321	0.267	15	15

Ontogeny and Photophore Arrangement

Based on the multivariate regression analyses and 2B-PLS, photophore arrangement is strongly correlated with standard length among the *Diaphus dumerilii* specimens in this study (Figure 8). Figure 8 shows the standard length against the regression scores of the multivariate regression. The regression score acts as a measure of the shape change per unit of size increase, which allows for a graphical representation of whether the shape changes of the photophores are constant or potentially slowing down as the size increases (Drake and Klingenberg, 2008). This is true of every regression and 2B-PLS of standard length versus the Procrustes coordinates and the first two PCs (Tables 7, 8). Photophore position also strongly correlates with nasal rosette diameter. This was confirmed by all regression and 2B-PLS tests conducted on the variable and most likely means nasal rosette diameter follows an allometric relationship with photophore arrangement. Head length and rosette diameter was also confirmed to follow an allometric

relationship with photophore arrangement, as confirmed by the additional regressions and 2B-PLS tests run on the first two PCs.

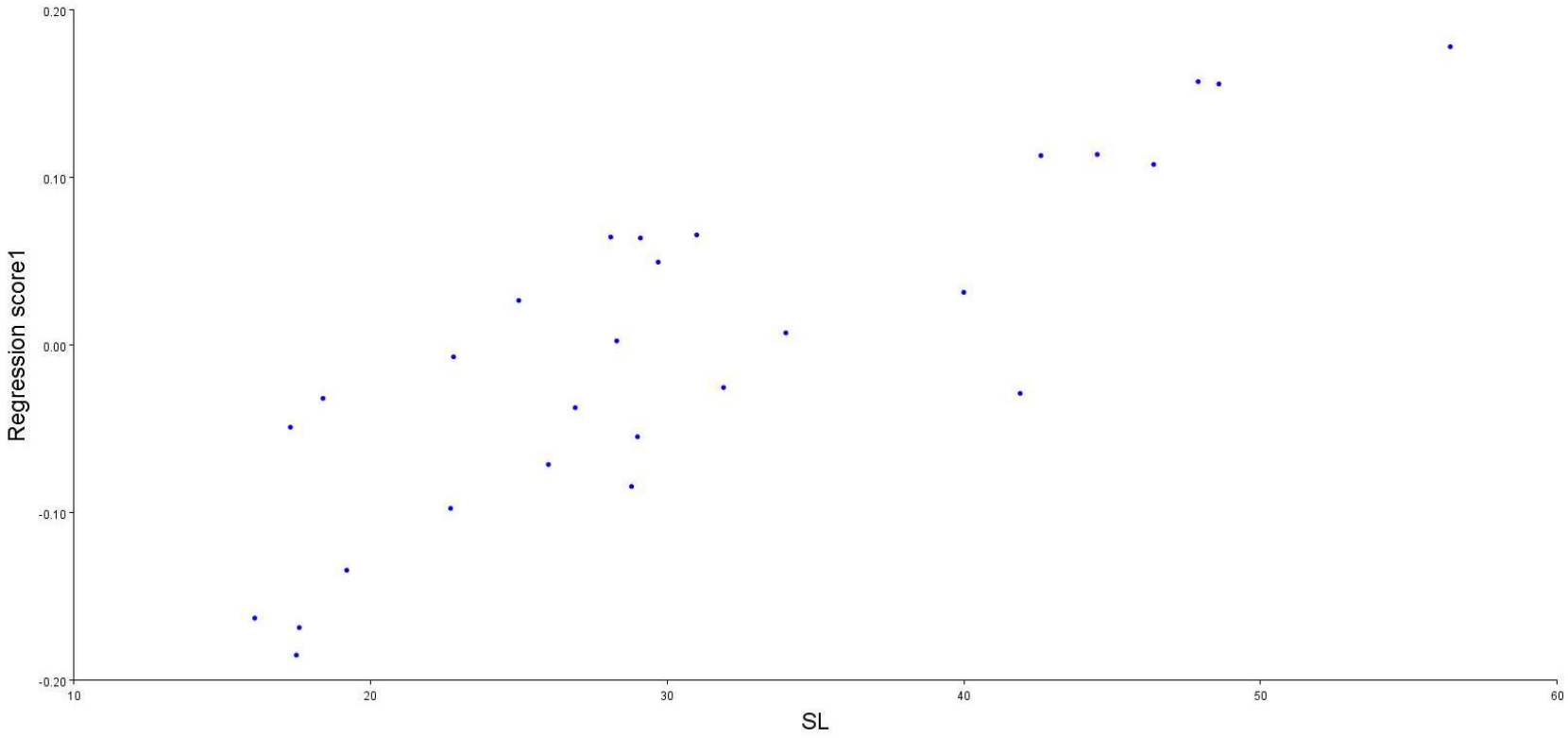

Figure 8 - Multivariate regression between Procrustes coordinates regression scores and standard length. Regression scores represent all observations in the sample.

Table 7 - Relationship between standard length and photophore arrangement of *Diaphus dumerilii* based on the multivariate regression. Significant p-values are in bold.

	P-value	**Total SS**	**Predicted SS**	**Residual SS**	**Percent Predicted**
Standard Length:					
Procrustes Coordinates	**<0.0001**	0.9186	0.0023	0.5488	40.25%
PC1	**<0.0001**	0.5655	0.3063	0.2592	54.16%
PC2	**0.0011**	0.3530	0.0634	0.2896	17.96%

Table 8 - Relationship between standard length and photophore arrangement of *Diaphus dumerilii* based on the 2B-PLS. Significant p-values are in bold.

	P-value	**RV Coefficient**	**Correlation**
Procrustes Coordinates	**<0.0001**	0.5546	0.8359
PC1	**<0.0001**	0.5417	0.7359
PC2	**0.0015**	0.1796	0.4237

Outline Analysis

Nasal Rosette Outlines

Seventeen nasal rosette outlines were created and assessed visually using a panel plot in the Momocs package (R software; Figure 9).

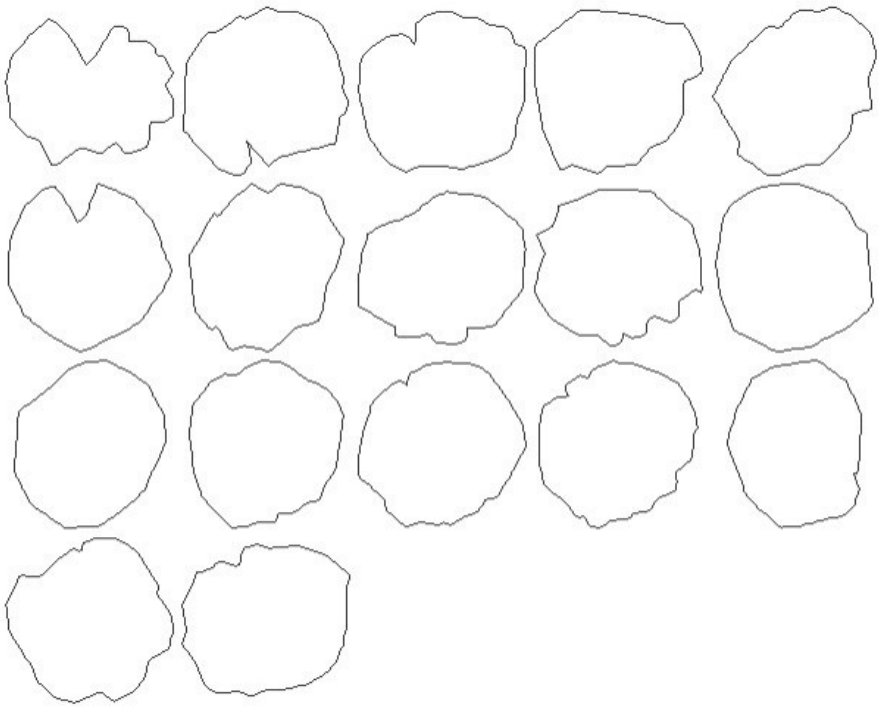

Figure 9 - Panel of the 17 manually created nasal rosettes used for outline analysis.

Shape Scalar Regressions

The results of the linear regressions on the relationship between standard length and the scalars (derived from the rosette outlines) are shown in Table 9 and Figure 10. For the nasal rosettes, there was a significant relationship between the SL and the area, caliper length, centroid size, circularity, Haralick circularity, and solidity ($p<0.05$). The scalar descriptors that were significant tended to be the ones that described the size and circularity of the rosettes (Table 9; Figure 10).

Table 9 - Summary of linear regression variables and potential significance for nasal rosette scalars against the log-transformed standard length (SL). Scalar = m*(log(SL)) + b.

Scalar	*m*	*b*	R^2	*p*
Area	80818	-232583	0.915	**<0.05**
Caliper Length	223.95	-510.24	0.937	**<0.05**
Centroid Size	105.28	-245.96	0.932	**<0.05**
Circularity	-3.188	27.948	0.201	**<0.05**
Haralick Circularity	9.025	-18.532	0.279	**<0.05**
Convexity	0.00957	0.8170	-0.06	0.779
Eccentricity Bounding Box	0.06201	0.6678	0.028	0.245
Elongation	-0.06201	0.3323	0.028	0.245
Rectangularity	0.04800	0.5656	0.150	0.069
Solidity	0.0506	0.7823	0.248	**<0.05**

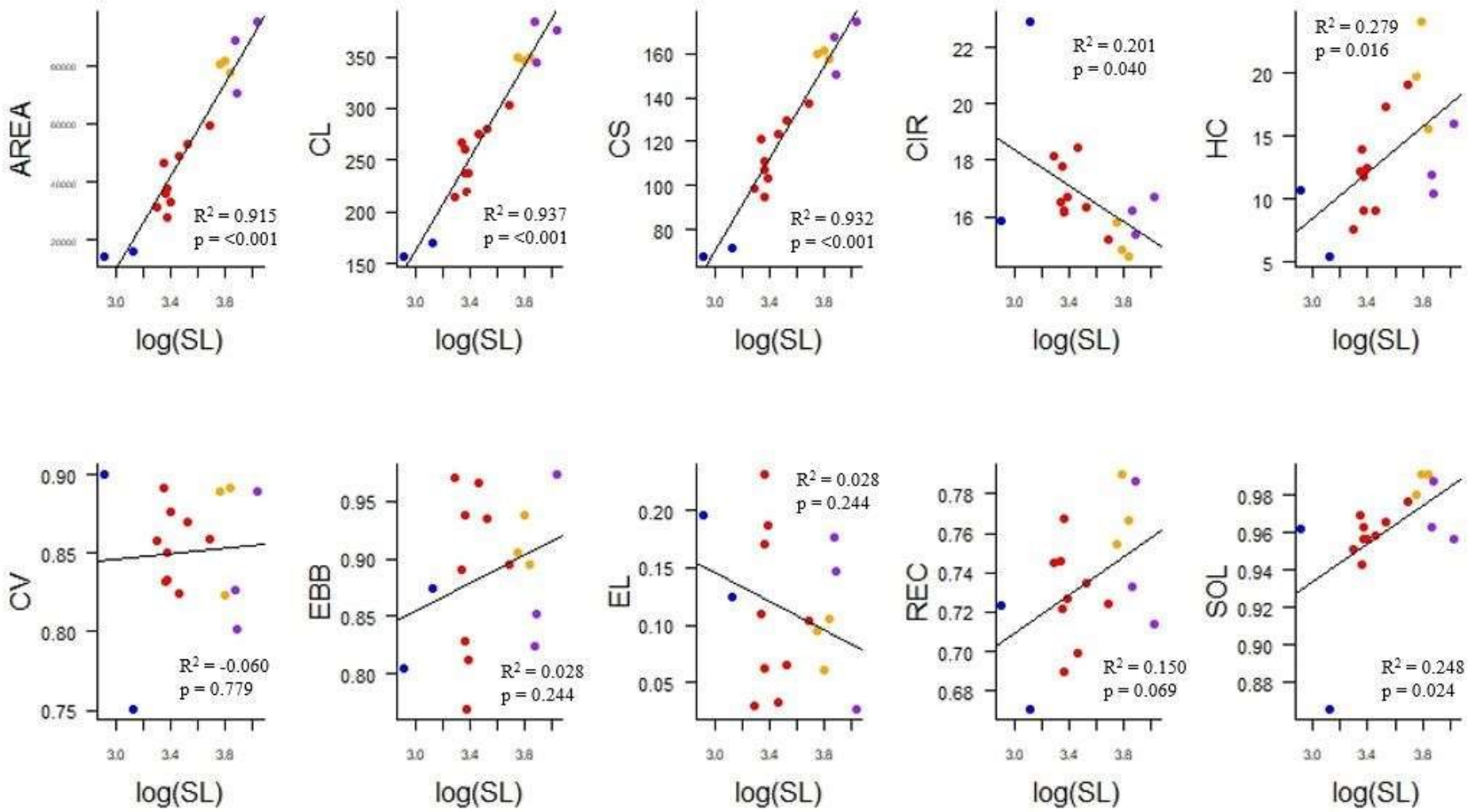

Figure 10 - Linear regressions between the log-transformed standard length and scalars for the nasal rosette outlines. Blue = Juveniles, Red = Maturing, Orange = Female, and Purple = Mature Male.

Maturity and Scalars

The one-way ANOSIM (with 10000 permutations) confirmed that the shape of the nasal rosettes (based on scalars) significantly differed between presumed maturity levels (Global R Statistic = 0.577, p-value = 0.002). The strongest difference between significant groups was between the juveniles and the maturing specimens (R Statistic = 0.646, p-value = 0.0036). There was also a significant difference between females and maturing specimens (R Statistic = 0.531, p-value = 0.005), and maturing and mature males (R Statistic = 0.576, p-value = 0.009; Table 10). The pairwise tests indicated that there was no significance between the mature males and females (R Statistic = 0.333, p-value = 0.20), juveniles and females (R Statistic = 0.833, p-value = 0.10), and juveniles and mature males (R Statistic = 0.833, p-value = 0.10; Table 10).

Table 10 - Pairwise test results from the ANOSIM run on the shape scalars and maturity level of the specimens. Significant p-values (<0.05) are in bold.

Groups	**R Statistic**	**P-values**	**Possible Permutations**	**Actual Permutations**
Juvenile, Maturing	0.646	**0.036**	55	55
Juvenile, Female	0.833	0.100	10	10
Juvenile, Mature Male	0.833	0.100	10	10
Maturing, Female	0.531	**0.005**	220	220
Maturing, Mature Male	0.576	**0.009**	220	220
Female, Mature Male	0.333	0.200	10	10

The PCA for the nasal rosette scalars indicates that PC1 and PC2 make up 75.8% of the cumulative variation in the shape of the organ (Figure 11). Centroid size (CS; correlation to axis = 0.398) and area (correlation to axis = 0.389) had the highest absolute values for PC1. The scalars were positively correlated, both increasing together. Eccentricity bounding box (EBB; correlation to axis = -0.575) and elongation (EL; correlation to axis = 0.575) had the highest absolute values for PC2. EBB was negatively correlated with EL, with EBB decreasing as EL increased.

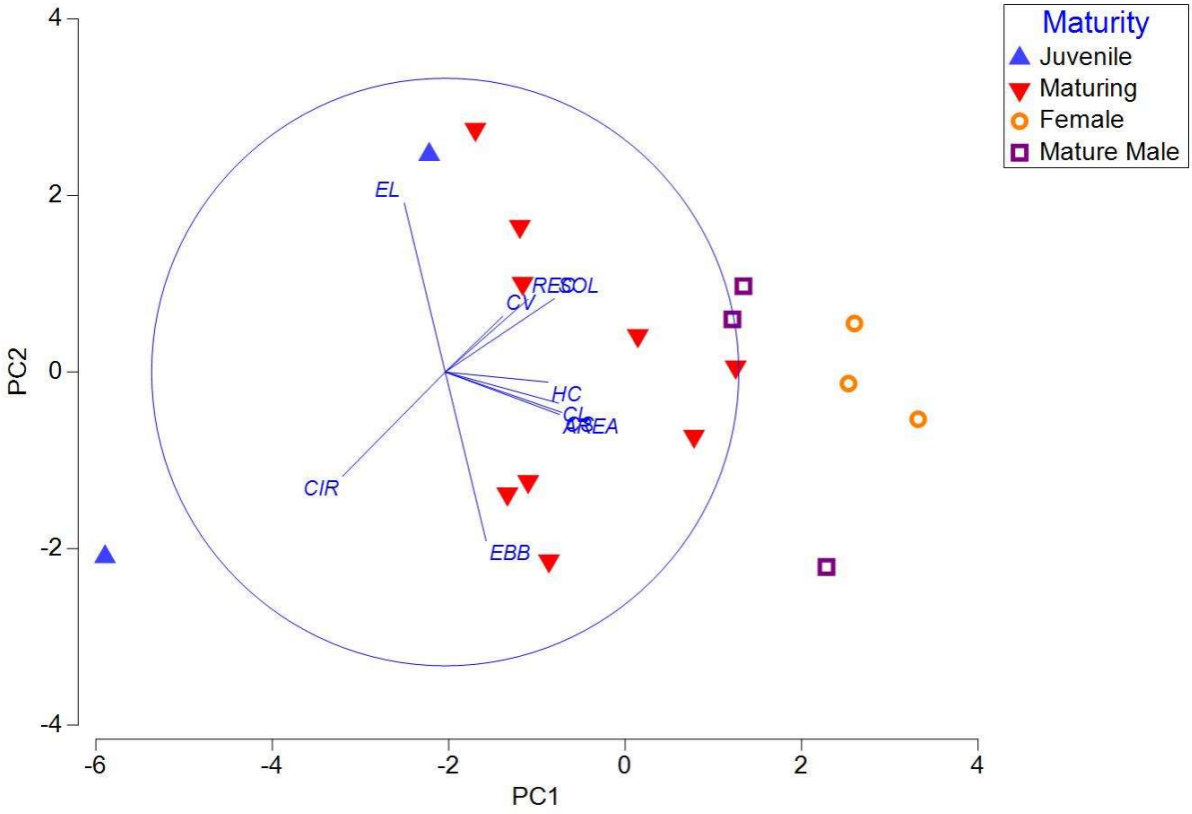

Figure 11 - Normalized PCA of nasal rosette scalars and maturity. Caliper length (CL), centroid size (CS), circularity (CIR), haralick circularity (HC), convexity (CV), eccentricity bounding box (EBB), elongation (EL), rectangularity (REC), and solidity (SOL).

Results from the hierarchical cluster analysis with SIMPROF show five homogenous groupings among the specimens based on the nasal rosette scalars (Figure 12). The first group consists of fish Ddum10, Ddum14, Ddum07, and Ddum13 with all but Ddum14 being maturing specimens. This is also the only group that has more than one maturity level within it. The second group consists solely of the maturing specimens Ddum11, Ddum04, and Ddum15. The mature males Ddum27 and Ddum29 were both grouped together, with the last mature male, Ddum28, being significantly different from the other specimens. Female specimens Ddum20 and Ddum24 were grouped together and maturing specimens Ddum26, Ddum21, and Ddum06 were all in the same group. Specimen Ddum01 was in a completely different group from every other specimen and may be an outlier.

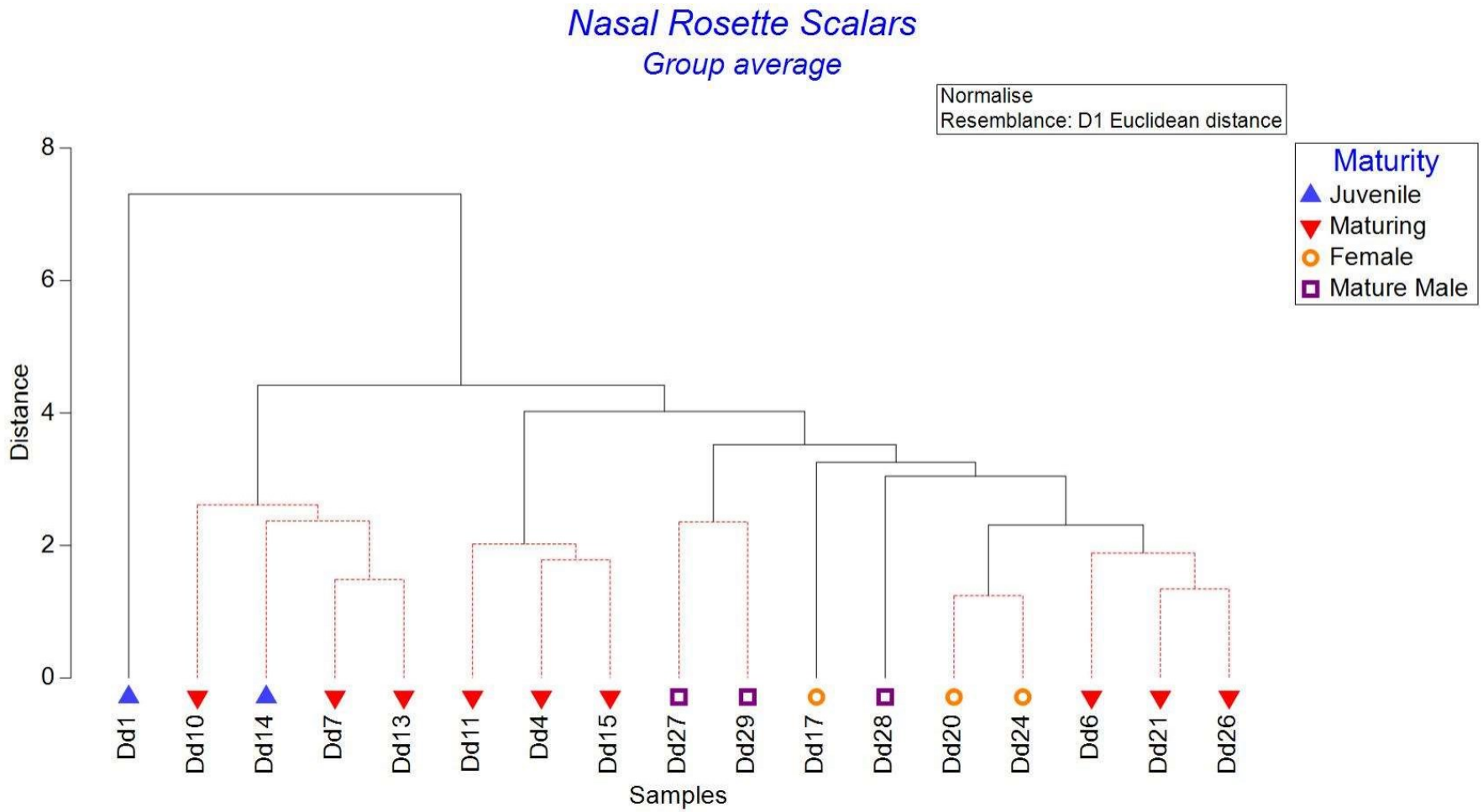

Figure 12 - Hierarchical cluster analysis with SIMPROF test of the nasal rosette scalars from the outlines of the *D. dumerilii* specimens.

Discussion

In this study, the phenotypic variation among the sensory organs of *Diaphus dumerilii* was examined via computer-aided morphometrics. The position of the photophores and size and shape of the nasal rosettes of *D. dumerilii* were examined and compared to body size via allometric indicators including inferred maturity, standard length, head length, and nasal rosette diameter. Morphometric analyses determined that photophore arrangement and nasal rosette size and shape were generally significantly associated with the body size of the individual. Among the two sensory features, the size of the features increased linearly with body size and inferred maturity. ANOSIM results indicated that while photophore arrangement and nasal rosette morphology was significantly associated with body size and inferred maturity, they were not significantly different between sexes. These findings suggest that these features may be playing different roles as the organisms develop, with potential differences related to the life stages or maturation of the individuals.

Diaphus samples

From a total of 28 individuals, four inferred maturity levels (juvenile, maturing, female, and mature male) were identified in this study. The overall size range of the specimens (16.1 – 56.4 mm) followed what other studies have found to encompass the standard range of the species from juveniles to adults (Gartner, 1991; Czudaj et al., 2022). Specimen collection was also comparable to the 3 mm mesh size used by DEEPEND, with Gartner (1991) and Czudaj et al., (2022) utilizing a 1.8 mm mesh. Log standard length (SL) and head length (HL) were strongly correlated with each other (cor. coef = 0.971), and both correlated with rosette diameter (RD; cor. coef = 0.925 and 0.927 respectively). The relationships between all three variables always showed a positive curvilinear correlation with each other (Figure 4). This implies that all three of these features (SL, HL, and RD) are growing at a similar rate. These are the first morphometric ratios between standard length, head length, and rosette diameter to be reported on *Diaphus dumerilii*. These relationships are important as it allows for inferring morphometric data from potentially missing measurements. A specimen with a damaged nasal rosette or head could still yield HL or RD information from the SL based on the ratios gathered from this study.

Photophore Arrangement

All landmark analyses determined that the photophore arrangement of the dorsonasal and ventronasal photophores in *Diaphus dumerilii* were significantly correlated with standard length and head length. The differences in photophore arrangement with growth appeared to become less prominent among mature specimens, as the ANOSIM results indicated that there was no significant difference in photophore arrangement between the mature males and females. There was also no significant difference between the maturing specimens and the mature specimens. The R statistic (indicating the degree of overlap) between groups of older, larger specimens (male and female) and juveniles was always greatest (Table 6). From the multivariate regressions and 2B-PLS tests, the photophore arrangement changed linearly and continuously with standard length (Figure 8), but not between mature males and females. While Dn and Vn photophore sizes are known to be sexually dimorphic, these results point towards head photophore arrangement potentially being a growth-related change only. As the photophore arrangement is not significantly different between sexes, it is possible they are not used for sexual selection and could be primarily a hunting tool or for interspecific identification (Haddock et al., 2010). Alternatively, the lack of apparent sexual selection could mean both sexes are utilizing photophore arrangement equally. If the primary purpose of the head photophores is for hunting, then there would be no need for sexual differences in the Dn and Vn arrangement as hunting is performed by males and females (Haddock et al., 2010).

The wireframe figure indicates that the dorsonasal photophore showed the most variation among specimens (Figure 6). Among *Diaphus dumerilii*, the size of the dorsonasal photophore is considered the primary indicator of sexual dimorphism, with it being larger among males (Sutton et al., 2020a). The secondary mark of sexual dimorphism in *D. dumerilii* is the bright yellow luminous patch located between the dorsonasal photophore and the eye in mature males (Nafpaktitis, 1968; Cavallaro et al., 2016). The relatively large variation in the dorsonasal landmark observed here is most likely due to the size variation of the organ shown by the species via sexual dimorphism, such as the luminous patch getting bigger in males. As the luminous patch becomes larger, it appears to push the dorsonasal photophore more towards the front of the head (Cavallaro et al., 2016). As both of these sensory features are sexually dimorphic (in mature individuals), the region on the head in which the landmark was placed would most likely show the most variation. The variation in the Dn photophore landmark makes the ANOSIM results of

no significance between mature male and female photophore arrangement unexpected. One explanation could be because the ANOSIM is describing the total variation among the three landmarks, not just the variation of the Dn position. The Vn and jaw are not sexually dimorphic among *D. dumerilii*, so they could be hiding the potential Dn variation in the overall landmark configuration. The relatively small sample size of mature specimens or a potential mislabeling of maturity among some specimens could also be influencing the ANOSIM results. A larger sample size and definitive sexing of the specimens would grant further insight into what may be causing the lack of significance.

Nasal Rosettes

Nasal rosette diameter was strongly correlated with standard length ($R^2 = 0.849$), head length ($R^2 = 0.853$), and photophore position ($R^2 = 0.778$; Figure 4, 10). Nasal rosette growth among *Diaphus* species is relatively unknown, but strong correlations with standard length have been observed in pelagic and deep-sea taxa, such as deep-sea lizardfishes (Synodontidae), and in salmonids, which show allometric growth (Fishelson et al., 2010; Rheinsmith et al., 2023).

Results from the scalar descriptors of rosette shape confirmed that all size-related descriptors such as area, caliper length, and centroid size were significantly correlated with standard length, with the scalars increasing as the standard length increased. The relationship among the size descriptors was always a positive curvilinear increase with log standard length (Figure 10). This further supports nasal rosettes displaying allometric growth among the specimens along with the nasal rosette diameter showing strong correlation with standard length. In deep-sea lizardfishes, rosette diameter appears to reach a maximum, species-specific length upon adulthood (Fishelson et al., 2010), while in salmonids the rosette size continues to increase throughout their lives (Rheinsmith et al., 2023). This study included several mature *D. dumerilii* specimens and the rosette diameter continued to increase even once the specimens were past maturity, suggesting indeterminate growth being more likely, but a larger sample size of mature specimens would be a more definitive indicator.

In terms of shape descriptors, circularity, Haralick circularity, and solidity were all significantly associated with standard length. Haralick circularity and solidity increased with increasing length, and circularity decreased with increasing length. An increasing solidity

measure with standard length means that the nasal rosettes of juveniles could potentially be more "jagged" or irregular in shape than when they begin to mature. An increasing Haralick circularity value supports this possibility as the nasal rosettes become more circular and "solid" as the specimens age. A possible explanation for this increased circularity and solidity among the nasal rosettes is that the number of lamellae within the rosettes may be increasing as well. It has been well documented that among many fish species, the number of lamellae within the rosettes increases as fish mature (Kasumyan, 2004; Fishelson et al., 2010; Rheinsmith et al., 2023). As more lamellae form within the rosette in maturing specimens, the overall shape of the structure may begin to "round out". The increase in size, and potentially increase in number of lamellae, of the nasal rosettes as the fish mature could mean the olfactory ability of *D. dumerilii* is increasing as well (Kumari, 2008). In nasal rosettes, increases in surface area have shown correlation with greater olfactory efficiency (Kumari, 2008). As a morphotype B species of *Diaphus*, *D. dumerilii* have generally smaller eyes than morphotype A species (de Busserolles et al., 2013). Wagner (2002) reported that in mesopelagic fishes, species with reduced optic tectum in the brain, typically had larger olfactory organs. Myctophids have been documented to have sub-average or even reduced optic tecta (Wagner, 2002), which could place more emphasis on olfaction, especially considering the already reduced eye size of morphotype B myctophids. The role of olfaction in *Diaphus dumerilii* is still a relative unknown, but future works looking into whether morphotype B species generally have larger olfactory organs than morphotype A could yield interesting insight into the importance of olfaction among the *Diaphus* genus.

ANOSIM and cluster analysis results revealed significant relationships between nasal rosette diameter and SL and inferred maturity. The nasal rosette shape scalars showed that the shape of the rosette was significantly different between juveniles to maturing and maturing to mature males and females. Considering the allometric relationship nasal rosette diameter has with standard length and evidence suggesting larger nasal rosettes are more efficient (Kumari, 2008), juveniles may have less of a need for a strong olfactory sense. These results would support the primary use of olfaction in *D. dumerilii* being for sexual selection or mate location, as juveniles would have no need for these functions. Juveniles were found to not be significantly different from mature males and females, but this is most likely due to the small sample size of available specimens for all four maturity levels. Considering the p-value was as small as it could have been from the possible permutations (10 permutations allow a minimum p-value of 0.10),

juveniles may be significantly different from mature males and females as well. The high R Statistic between the three groups suggests strong dissimilarity (R = 0.833). The low dissimilarity and lack of significance between the mature males and females is most likely due to a lack of sexual dimorphism in the nasal rosettes of *Diaphus dumerilii*. However, lack of sexual dimorphism does not necessarily mean there is no mate selection taking place, especially considering mesopelagic organisms generally do not display sexual dimorphism in their nasal rosettes (Priede, 2017). If both sexes possess the same size nasal rosette, it could indicate that mate selection or pheromone detection is equally important among male and female *D. dumerilii*. It has been proposed that since pheromone detection largely outranges visual capabilities in myctophids, eyes alone would be unable to determine species-specific patterning in photophores at large distances and would only be useful in tandem with other sensory mechanisms (such as chemoreception; Herring, 2000).

Caveats and Future Considerations

For future studies that may examine phenotypic variability through a computer-aided lens, there are certainly further aspects to consider. The first is that while the specimens utilized for this study were relatively recently obtained, any amount of time in preservative such as 70% ethanol can alter morphological characteristics (Moku et al., 2004). Moku et al. (2004) found that the body lengths of *Diaphus* larvae preserved in 70% ethanol decreased by 2.4% in only one week of exposure to the solution. It has also been reported that different species of fish can be affected by fixatives at different magnitudes (Jawad et al., 2020). Jawad et al., (2020) found that different cichlid species had decreases in SL and HL at different rates to each other when preserved in formalin and ethanol. Freezing the specimens resulted in the least amount of distortion between species. Martinez et al., (2013) have found that fixatives can even alter geometric morphometric analyses. When performing Procrustes ANOVAs, discriminant analyses, and PCAs, there were significant differences in shape variation between the same specimens before and after they were preserved in formalin (Martinez et al., 2013). Martinez et al., (2013) did not test the effects of freezing but considering freezing has been reported to show the least amount of distortion, that could be an alternative to placing the specimens in formalin (Jawad et al., 2020). However, in order to get the most accurate morphometric data possible,

specimens should be measured before transfer to a preservative, if possible. Performing observations and measurements on fresh specimens would most likely yield the least distorted results.

Future works looking at visual sensory systems on top of photophore arrangement and olfaction could potentially explain more of the sensory variation. Eye size is a sensory organ characteristic that is also known to scale allometrically with body size among myctophids and is also essential to hunting and finding mates (de Busserolles et al., 2013). Eye-size variability has been described for numerous *Diaphus* species (e.g., *D. mollis, D. garmani, D. holti*, and *D. meadi*), with findings that organisms without a So-photophore tend to have smaller eyes (de Busserolles et al., 2013). Eye-size variability among *D. dumerilii* has not been documented, however *D. dumerilii* is a morphotype B species lacking a So-photophore, making it likely this trend follows the same for the species. The fact that the presence or absence of photophores can influence other head sensory characteristics like eye size, indicates these features may be correlated, with fish possessing larger eyes potentially being less reliant on photophores or olfaction. In the same way sensory capabilities are influenced by eye size, dorsonasal and ventronasal photophore arrangement could be sensory features that shows allometric growth due to the organs becoming more important as the myctophids mature (de Busserolles et al., 2013).

While conducting the landmark analyses, duplicate images were taken to minimize the potential human error in placing the landmarks in incorrect positions. While the Procrustes ANOVA confirmed that digitization error was not significant, human error is still a possibility in any study that requires the manual placement of landmarks. There is also some contention on how many landmarks should be utilized to fully represent a feature. A computational tool called the Landmark Sampling Evaluation Curve (LaSEC) has been created to assess how many landmarks are needed to represent a shape without under- or oversampling landmarks (Watanabe, 2018). Using this tool, Watanabe (2018) suggested that at a minimum, the number of landmarks placed on each specimen should exceed the total number of specimens to most accurately represent shape and size data but should still be considered in a case-by-case basis (Watanabe, 2018). In this case, this approach was not possible due to the number of features being biologically limited, but other studies have used a smaller number of landmarks (3-5) when describing features with limited points for placement (e.g., photophores) and have yielded

good results (Davis et al., 2014). A potential future study could landmark not only the photophores, but also other morphologically distinct features such as the operculum, eye, or maxilla to determine which features are most affected by ontogeny. With more landmarked points, wireframe results could indicate if the Dn and Vn show more variation than other features known to scale with allometry.

While digitization error was low for the landmark analysis, digitization noise of the outlines is a possible explanation as to why circularity was negatively associated with standard length, but Haralick circularity was not (Rosin, 2005). An uneven or "noisy" perimeter around an object can cause measuring overestimations that can lead to incorrectly describing circular objects as non-circular (Rosin, 2005). Haralick circularity gets around this by determining circularity as distances from the center and any point on the perimeter, leading to the centroid of the shape being the object considered circular (Rosin, 2005). This could be likened to using the area of an object to measure circularity as opposed to the perimeter. Any potential digitization noise or nasal rosette degradation could lead to a nasal rosette being declared non-circular by the circularity descriptor, but circular by the Haralick circularity descriptor.

Several of the smaller *D. dumerilii* also had damaged or degraded nasal rosettes which led to many of them being excluded from the scalar descriptor analyses. The sample size of specimens that had intact nasal rosettes compared to the number of landmarked specimens was much smaller, however there were still significant results from the ANOSIM and cluster analysis. A potential reason for the large number of juveniles with damaged or degraded rosettes could be that the net used to collect the specimens, damages the smaller specimens more. Another possibility is that formalin used to preserve the specimens, has a greater distortion effect on the developing nasal rosettes of juvenile fish.

By performing outline analyses in this study, shape variation of the nasal rosette outlines could be utilized to give insight into what underlying mechanisms or factors may be influencing the shape of the nasal rosettes of *D. dumerilii* (Bonhomme et al., 2014). A limitation of these outlines, however, is that they are two-dimensional shapes describing three-dimensional objects. Nasal rosettes, in particular, are made up of several petal-like folds called lamellae that make up the whole rosette (Fishelson et al., 2010). Since the silhouettes created from the outlines do not account for variation inside the shape, lamellae information is lost. A potential 3D rendering, or

scan of the nasal rosettes would be able to capture both the outer shape variation, as well as potential lamellae variation within the rosette. Variance due to sexual dimorphism is another aspect that can be considered. Sex has been determined in *D. dumerilii* in specimens as small as 24 mm SL (Gartner, 1993) through dissections, which were not able to be performed during this study, hence the use of inferred sex and maturity levels. In order to potentially have clearer separation between males and females, maturing individuals could be dissected to give greater insight to how sex may play a part in sensory development. Dissection could also give further insight into the maturity levels of the individuals. In this study based on the SL, there were no fully mature female specimens. The only way to truly confirm this would be to age the organisms through dissection.

Conclusion

Both sensory systems examined in this study (head photophores and nasal rosettes) showed significant relationships with maturity/body length. Based on the landmarked points, head photophore arrangement changed linearly with maturity level but showed no significant difference between sexes. Between the Dn and Vn photophore, the Dn showed more variation, potentially due to the presence of the large, luminous antorbital patch present in mature males. Nasal rosette size was also significantly associated with maturity level but not with sex. Differences in nasal rosette shape were only significant between a few maturity levels, but limitations in the number of intact rosettes in the smaller individuals is most likely the cause of this. The presence of both species-specific photophores and well-developed olfactory organs in *D. dumerilii* raises the question of how important visual versus olfactory cues are for the species at different life stages. Evidence for allometric changes in both photophore arrangement and nasal rosette morphology indicates that both roles of these organs may be changing throughout the organisms' lives. Olfaction could assist in mate location during some stages of an organisms' life, while photophore arrangement could primarily be used for interspecific identification, however, until more research is conducted on the morphology of sensory systems and their roles in *D. dumerilii* this is still a relative unknown. The main findings of this study highlight the need for morphometric analyses on understudied organisms such as *D. dumerilii,* as even the use of

preserved specimens can be used to infer new information on the life history and behavioral ecology of a species that cannot be reliably observed in their natural environment.

References

Anumudu C.I., and Mojekwu, T. (2015). Advanced techniques for morphometric analysis in fish. Journal of Aquaculture Research and Development, 6(8). https://doi.org/10.4172/2155-9546.1000354

Baird, R., Johari, H., and Jumper, G. (1996). Numerical simulation of environmental modulation of chemical signal structure and odor dispersal in the open ocean. Chemical senses, 21, 121-134. https://doi.org/10.1093/chemse/21.2.121

Baird, R.C., Jumper, G.Y., and Gallaher, E.E. (1990). Sexual dimorphism and demography in two species of oceanic midwater fishes (Stomiiformes: Sternoptychidae) from the eastern Gulf of Mexico. Bulletin of Marine Science, 47(2), 561-566.

Bangma, J.L., and Haedrich, R.L. (2008). Distinctiveness of the mesopelagic fish fauna in the Gulf of Mexico. Deep Sea Research Part II: Topical Studies in Oceanography, 55(24), 2594-2596. https://doi.org/https://doi.org/10.1016/j.dsr2.2008.07.008

Battaglia, P., Esposito, V., Malara, D., Falautano, M., Castriota, L., and Andaloro, F. (2014). Diet of the spothead lanternfish *Diaphus metopoclampus* (Cocco, 1829) (Pisces: Myctophidae) in the central Mediterranean Sea. Italian Journal of Zoology, 81(4), 530-543. https://doi.org/10.1080/11250003.2014.948500

Begg, G.A., and Waldman, J.R. (1999). An holistic approach to fish stock identification. Fisheries Research, 43(1-3), 35-44. https://doi.org/10.1016/s0165-7836(99)00065-x

Bernard, A.M., Finnegan, K.A., Sutton, T.T., Eytan, R.I., Weber, M.D., and Shivji, M.S. (2022). Population genomic dynamics of mesopelagic lanternfishes *Diaphus dumerilii*, *Lepidophanes guentheri*, and *Ceratoscopelus warmingii* (Family: Myctophidae) in the Gulf of Mexico. Deep Sea Research Part I: Oceanographic Research Papers, 185, 103786. https://doi.org/https://doi.org/10.1016/j.dsr.2022.103786

Bolin, R. (1959). Iniomi (myctophidae Exclusive), Lyomeri, Apodes from the "Michael Sars" North Atlantic Deep- Sea Expedition 1910. John Grieg. https://books.google.com/books?id=ZyXAngEACAAJ

Bonhomme, V., Picq, S., Gaucherel, C., and Claude, J. (2014). Momocs: outline analysis using R. Journal of Statistical Software, 56(13), 1 - 24. https://doi.org/10.18637/jss.v056.i13

Boughman, J.W. (2002). How sensory drive can promote speciation. Trends in Ecology and Evolution, *17*(12), 571-577. https://doi.org/https://doi.org/10.1016/S0169-5347(02)02595-8

Cadrin, S.X., and Friedland, K.D. (1999). The utility of image processing techniques for morphometric analysis and stock identification. Fisheries Research, 43(1-3), 129-139. https://doi.org/10.1016/s0165-7836(99)00070-3

Caillon, F., Bonhomme, V., Möllmann, C., and Frelat, R. (2018). A morphometric dive into fish diversity. Ecosphere, 9(5), e02220. https://doi.org/10.1002/ecs2.2220

Cavallaro, M., Ammendolia, G., Andaloro, F., and Battaglia, P. (2016). First record of the mesopelagic fish *Diaphus dumerilii* (Bleeker, 1856) in the Mediterranean Sea. Marine Biodiversity, 47, 585-588. https://doi.org/10.1007/s12526-016-0492-3

Claes, J.M., and Mallefet, J. (2009). Ontogeny of photophore pattern in the velvet belly lantern shark, *Etmopterus spinax*. Zoology, 112(6), 433-441. https://doi.org/https://doi.org/10.1016/j.zool.2009.02.003

Claes, J.M., Nilsson, D.E., Straube, N., Collin, S.P., and Mallefet, J. (2015). Iso-luminance counterillumination drove bioluminescent shark radiation. Scientific Reports, 4(1). https://doi.org/10.1038/srep04328

Clarke, W.D. (1963). Function of bioluminescence in mesopelagic organisms. Nature, 198(4887), 1244-1246. https://doi.org/10.1038/1981244a0

Clarke, K.R. and Gorley, R.N. (2015). PRIMER v7: user manual/tutorial. PRIMER-E, Plymouth

Cook, A.B., Bernard, A.M., Boswell, K.M., Bracken-Grissom, H., D'Elia, M., deRada, S., Easson, C.G., English, D., Eytan, R.I., Frank, T., Hu, C., Johnston, M.W., Judkins, H., Lembke, C., Lopez, J.V., Milligan, R.J., Moore, J.A., Penta, B., Pruzinsky, N.M., Quinlan, J.A., Richards, T.M., Romero, I.C., Shivji, M.S., Vecchione, M., Weber, M.D., Wells, R.J.D., and Sutton, T.T. (2020). A multidisciplinary approach to investigate deep-pelagic ecosystem dynamics in the Gulf of Mexico following Deepwater Horizon [methods]. Frontiers in Marine Science, 7. https://doi.org/10.3389/fmars.2020.548880

Czudaj, S., Möllmann, C., and Fock, H.O. (2022). Length–weight relationships of 55 mesopelagic fishes from the eastern tropical North Atlantic: across- and within-species variation (body shape, growth stanza, condition factor). Journal of Fish Biology. https://doi.org/10.1111/jfb.15068

Davis, M.P., Holcroft, NI., Wiley, E.O., Sparks, J.S., and Leo S.W. (2014). Species-specific bioluminescence facilitates speciation in the deep sea. Marine Biology, 161(5), 1139-1148. https://doi.org/10.1007/s00227-014-2406-x

de Busserolles, F., Fitzpatrick, J., Paxton, J., Marshall, N., and Collin, S. (2013). Eye-size variability in deep-sea lanternfishes (Myctophidae): an ecological and phylogenetic study. PLoS ONE, 8, e58519. https://doi.org/10.1371/journal.pone.0058519

de Busserolles, F., and Marshall, N.J. (2017). Seeing in the deep-sea: visual adaptations in lanternfishes. Philosophical Transactions of the Royal Society B: Biological Sciences, 372(1717), 20160070. https://doi.org/10.1098/rstb.2016.0070

Denton, J.S.S. (2014). Seven-locus molecular phylogeny of Myctophiformes (Teleostei; Scopelomorpha) highlights the utility of the order for studies of deep-sea evolution. Molecular Phylogenetics and Evolution, 76, 270-292. https://doi.org/10.1016/j.ympev.2014.02.009

Duchatelet, L., Hermans, C., Duhamel, G., Cherel, Y., Guinet, C., and Mallefet, J. (2019). Coelenterazine detection in five myctophid species from the Kerguelen Plateau. Proceedings of the Second Symposium. Australian Antarctic Division, Kingston, Tasmania, Australia. ISBN: 978-1-876934-30-9. pp.31-41. https://archimer.ifremer.fr/doc/00502/61405/

Endler, J.A. (1992). Signals, signal conditions, and the direction of evolution. The American Naturalist, 139, S125 - S153.

Fishelson, L., Golani, D., Galil, B., and Goren, M. (2010). Comparison of the nasal olfactory organs of various species of lizardfishes (Teleostei: Aulopiformes: Synodontidae) with additional remarks on the brain. International Journal of Zoology, 807913. https://doi.org/10.1155/2010/807913

Frimpong, E., and Angermeier, P. (2010). Trait-based approaches in the analysis of stream fish communities. In American Fisheries Society Symposium (pp. 109-136). https://doi.org/10.13140/2.1.4590.7840

Fricke, R., Eschmeyer, W.N. and Fong, J.D. (2022) Species by family/subfamily. http://researcharchive.calacademy.org/research/ichthyology/catalog/SpeciesByFamily.asp.

Gartner, J.V., Hopkins, T.L., Baird, R.C., and Milliken, D.M. (1987). The lanternfishes (Pisces, Myctophidae) of the eastern Gulf of Mexico. Fisheries Bulletin, 85, 81-98.

Gartner, J.V. (1991). Life histories of three species of lanternfishes (Pisces: Myctophidae) from the eastern Gulf of Mexico. Marine Biology, 111(1), 21-27. https://doi.org/10.1007/bf01986340

Gartner, J.V. (1993). Patterns of reproduction in the dominant lanternfish species (Pisces: Myctophidae) of the eastern Gulf of Mexico, with a review of reproduction among the tropical-subtropical Myctophidae. Bulletin of Marine Science, 52(2), 721-750.

Gibert, J.P., Dell, A.I., Delong, J.P., and Pawar, S. (2015). Scaling-up trait variation from individuals to ecosystems. Advances in Ecological Research, 52, 1-17.

GIMP Development Team. (2022). GIMP. Retrieved from https://www.gimp.org.

Gjøsæter, J. and Tilseth, S. (1988). Spawning behavior, egg and larval development of the myctophid fish *Benthosema pterotum*. Marine Biology, 98(1), 1-6.

Gower, J.C. (1975). Generalized Procrustes analysis. Psychometrika, 40(1), 33-51. https://doi.org/10.1007/BF02291478

Haddock, S.H.D., Moline, M.A., and Case, J.F. (2010). Bioluminescence in the sea. Annual Review of Marine Science, 2(1), 443-493. https://doi.org/10.1146/annurev-marine-120308-081028

Haddock, S.H.D., Rivers, T.J., and Robison, B.H. (2001). Can coelenterates make coelenterazine? Dietary requirement for luciferin in cnidarian bioluminescence. Proceedings of the National Academy of Sciences, 98(20), 11148-11151. https://doi.org/doi:10.1073/pnas.201329798

Herring P.J. (2000). Species abundance, sexual encounter and bioluminescent signaling in the deep sea. Philosophical transactions of the Royal Society of London. Series B, Biological sciences, *355*(1401), 1273–1276. https://doi.org/10.1098/rstb.2000.0682

Herring, P.J. (2007). Sex with the lights on? A review of bioluminescent sexual dimorphism in the sea. Journal of the Marine Biological Association of the United Kingdom, 87(4), 829-842. https://doi.org/10.1017/s0025315407056433

Jawad, L., Koya, A., and Gnohossou, P. (2020). Fixation, preservation and freezing effects on morphometrics of two fish species collected from Lake Ganvie, Benin, West Africa. Thalassia Salentina, 42, 75-82.

Jochens, A.E., and DiMarco, S.F. (2008). Physical oceanographic conditions in the deepwater Gulf of Mexico in summer 2000-2002. Deep Sea Research Part II, 55(24), 2541-2554.

Jolliffe, I.T., and Cadima, J. (2016). Principal component analysis: a review and recent developments. Phil. Trans. of the Royal Soc., 374(2065), 20150202

Judkins, H., Vecchione, M., Cook, A., and Sutton, T. (2017). Diversity of midwater cephalopods in the northern Gulf of Mexico: comparison of two collecting methods. Marine Biodiversity, 47(3), 647-657. https://doi.org/10.1007/s12526-016-0597-8

Jumper, G.Y., and Baird, R.C. (1991). Location by olfaction: a model and application to the mating problem in the deep-sea hatchetfish *Argyropelecus hemigymnus*. The American Naturalist, 138(6), 1431-1458. http://www.jstor.org/stable/2462555

Kasumyan, A. (2004). The olfactory system in fish: structure, function, and role in behavior. Journal of Ichthyology, 44, S180-S223

Kiørboe, T., Visser, A., and Andersen, K.H. (2018). A trait-based approach to ocean ecology. ICES Journal of Marine Science, 75(6), 1849-1863. https://doi.org/10.1093/icesjms/fsy090

Klingenberg, C.P. (2011). MorphoJ: an integrated software package for geometric morphometrics. Molecular Ecology Resources, 11(2), 353-357. https://doi.org/10.1111/j.1755-0998.2010.02924.x

Kumari, K. (2009). Morphology and morphometry of the olfactory rosette of a teleostean fish: *Catla catla* (ham.). Our Nature, 6(1), 30-37

Lawry, J. V. (1973). The olfactory epithelium of the lantern fish, *Tarletonbeania crenularis* (Myctophidae). Zeitschrift für Zellforschung und Mikroskopische Anatomie, 138(1), 31-39. https://doi.org/10.1007/BF00307076

Lindo-Atichati, D., Bringas, F., Goni, G., Muhling, B., Muller-Karger, F., and Habtes, S. (2012). Varying mesoscale structures influence larval fish distribution in the northern Gulf of Mexico. Marine Ecology Progress Series, 463, 245-257. https://doi.org/10.3354/meps09860

Marshall, N.B. (1967). Olfactory organs of bathypelagic fishes. Symposia of the Zoological Society of London 19, 57-70

Martinez, C.M., Friedman, S.T., Corn, K.A., Larouche, O., Price, S.A., and Wainwright, P.C. (2021). The deep sea is a hot spot of fish body shape evolution. Ecology Letters, 24(9), 1788-1799. https://doi.org/10.1111/ele.13785

Martinez, P.A., Berbel-Filho, W.M., and Jacobina, U.P. (2013). Is formalin fixation and ethanol preservation able to influence in geometric morphometric analysis? Fishes as a case study. Zoomorphology, 132(1), 87-93.

Martini, S., Kuhnz, L., Mallefet, J., and Haddock, S. H. D. (2019). Distribution and quantification of bioluminescence as an ecological trait in the deep sea benthos. Scientific Reports, 9(1). https://doi.org/10.1038/s41598-019-50961-z

Mead, G.W., Bertelsen, E., and Cohen, D.M. (1964). Reproduction among deep-sea fishes. Deep Sea Research and Oceanographic Abstracts, *11*(4), 569-596. https://doi.org/https://doi.org/10.1016/0011-7471(64)90003-8

Mensinger, A.F., and Case, J. F. (1990). Luminescent properties of deep sea fish. Journal of Experimental Marine Biology and Ecology, 144(1), 1-15. https://doi.org/10.1016/0022-0981(90)90015-5

Milligan, R.J., and Sutton, T.T. (2020). Dispersion overrides environmental variability as a primary driver of the horizontal assemblage structure of the mesopelagic fish family Myctophidae in the northern Gulf of Mexico. Frontiers in Marine Science, 7. https://doi.org/10.3389/fmars.2020.00015

Moku, M., Mori., K., and Watanabe, Y. (2004). Shrinkage in the body length of myctophid fish (*Diaphus* slender-type spp.) larvae with various preservatives. Copeia, 2004(3), 647-651

Nafpaktitis, B.G. (1968). Taxonomy and distribution of the lanternfishes, genera *Lobianchia* and *Diaphus* in the North Atlantic. Dana Reports. 73, 1-131. https://ci.nii.ac.jp/naid/10022589919/en/

Nafpaktitis, B.G., Robertson, D.A., and Paxton, J.R. (1995). Four new species of the lanternfish genus *Diaphus* (Myctophidae) from the Indo-Pacific. New Zealand Journal of Marine and Freshwater Research, 29(3), 335-344. https://doi.org/10.1080/00288330.1995.9516668

Paitio, J., Yano, D., Muneyama, E., Takei, S., Asada, H., Iwasaka, M., and Oba, Y. (2020). Reflector of the body photophore in lanternfish is mechanistically tuned to project the biochemical emission in photocytes for counterillumination. Biochemical and

Biophysical Research Communications, 521(4), 821-826. https://doi.org/10.1016/j.bbrc.2019.10.197

Palumbi, S.R. (1994). Genetic divergence, reproductive isolation, and marine speciation. Annual Review of Ecology and Systematics, 25(1), 547-572. https://doi.org/10.1146/annurev.es.25.110194.002555

Park, P.J., Aguirre, W.E., Spikes, D., and Miyazaki, J.M. (2013). Landmark-based geometric morphometrics: what fish shapes can tell us about fish evolution. Proceedings of the Association for Biology Laboratory Education. 34, 361-371.

Paulus, E. (2021). Shedding light on deep-sea biodiversity—A highly vulnerable habitat in the face of anthropogenic change [Review]. Frontiers in Marine Science, 8. https://doi.org/10.3389/fmars.2021.667048

Priede, I. (2017). Deep-sea fishes: biology, diversity, ecology and fisheries. https://doi.org/10.1017/9781316018330

R Development Core Team. (2022). R: A Language and Environment for Statistical Computing. In R Foundation for Statistical Computing.

Rheinsmith, S.E., Quinn, T.P., Dittman, A.H., and Yopak, K.E. (2023). Ontogenetic shifts in olfactory rosette morphology of the sockeye salmon, *Oncorhynchus neka*. J. Morphol, 284(1), e21539.

Roff, D. (1993). Evolution of life histories: theory and analysis. Springer Science and Business Media.

Rohlf, F. J. (1990). Morphometrics. annual review of ecology and systematics, 21(1), 299-316. https://doi.org/10.1146/annurev.es.21.110190.001503

Rohlf, F.J., and Slice, D. (1990). Extensions of the Procrustes method for the optimal superimposition of landmarks. Systematic Zoology, 39(1), 40. https://doi.org/10.2307/2992207

Rohlf, F.J. (2015), The Tps series of software. Hystrix, 26, 1-4.

Rosin, P.L. (2005). Computing global shape measures. Handbook of Pattern Recognition and Computer Vision, 177-196

Ross, S.W., Quattrini, A.M., Roa-Varón, A.Y., and McClain, J.P. (2010). Species composition and distributions of mesopelagic fishes over the slope of the north-central Gulf of Mexico. *Deep Sea Research Part II: Topical Studies in Oceanography*, *57*(21), 1926-1956. https://doi.org/https://doi.org/10.1016/j.dsr2.2010.05.008

Savriama, Y. (2018). A step-by-step guide for geometric morphometrics of floral symmetry. Frontiers in Plant Science, 9.

Schwarzhans, W., and Carnevale, G. (2021). The rise to dominance of lanternfishes (Teleostei: Myctophidae) in the oceanic ecosystems: a paleontological perspective. Paleobiology, 47(3), 446-463. https://doi.org/10.1017/pab.2021.2

Srijaya, T.C., Pradeep, P.J., Mithun, S., Hassan, A., Shaharom, F., and Chatterji, A. (2010). A new record on the morphometric variations in the populations of horseshoe crab (*Carcinoscorpius rotundicauda* Latreille) obtained from two different ecological habitats of peninsular Malaysia. Our Nature, *8*(1), 204-211. https://doi.org/10.3126/on.v8i1.4329

Sutton, T.T., Frank, T., Judkins, H., and Romero, I.C. (2020). As gulf oil extraction goes deeper, who is at risk? Community structure, distribution, and connectivity of the deep-pelagic fauna. In et al. Scenarios and Responses To Future Deep Oil Spills. Springer, Cham. https://doi.org/10.1007/978-3-030-12963-7_24

Sutton, T.T., and Milligan, R.J. (2019). Deep-sea ecology. In Encyclopedia of Ecology (Second Edition), edited by B. Fath (pp. 35-45). Elsevier. https://doi.org/10.1016/b978-0-12-409548-9.11010-3

Sutton, T.T., Porteiro, F.M., Heino, M., Byrkjedal, I., Langhelle, G., Anderson, C.I.H., Horne, J., Søiland, H., Falkenhaug, T., Godø, O.R., and Bergstad, O.A. (2008). Vertical structure, biomass and topographic association of deep-pelagic fishes in relation to a mid-ocean ridge system. Deep Sea Research Part II: Topical Studies in Oceanography, 55(1-2), 161-184. https://doi.org/10.1016/j.dsr2.2007.09.013

Sutton, T.T., Wiebe, P.H., Madin, L., and Bucklin, A. (2010). Diversity and community structure of pelagic fishes to 5000m depth in the Sargasso Sea. Deep Sea Research Part II: Topical Studies in Oceanography, 57(24-26), 2220-2233. https://doi.org/10.1016/j.dsr2.2010.09.024

Sutton, T.T. H., P.A., Wienerroither, R. ; Zaera-Perez, D. ; Paxton, J.R. (2020). Identification guide to the mesopelagic fishes of the central and southeast Atlantic Ocean. FAO Species Identification Guide for Fishery Purposes. Rome, FAO. 2020. https://doi.org/https://doi.org/10.4060/cb0365en

Turan, C., Oral, M., Öztürk, B., and Düzgüneş, E. (2006). Morphometric and meristic variation between stocks of Bluefish (*Pomatomus saltatrix*) in the Black, Marmara, Aegean and northeastern Mediterranean Seas. Fisheries Research, 79(1-2), 139-147. https://doi.org/10.1016/j.fishres.2006.01.015

Turner, J.R., White, E.M., Collins, M.A., Partridge, J.C., and Douglas, R.H. (2009). Vision in lanternfish (Myctophidae): Adaptations for viewing bioluminescence in the deep-sea. *Deep Sea Research Part I: Oceanographic Research Papers*, *56*(6), 1003-1017. https://doi.org/https://doi.org/10.1016/j.dsr.2009.01.007

Tuset, V.M., Olivar, M.P., Otero-Ferrer, J.L., López-Pérez, C., Hulley, P.A., and Lombarte, A. (2018). Morpho-functional diversity in *Diaphus* spp. (Pisces: Myctophidae) from the central Atlantic Ocean: Ecological and evolutionary implications. Deep Sea Research

Part I: Oceanographic Research Papers, 138, 46-59. https://doi.org/10.1016/j.dsr.2018.07.005

Véron, M., Duhamel, E., Bertignac, M., Pawlowski, L., Huret, M., and Baulier, L. (2020). Determinism of temporal variability in size at maturation of sardine *Sardina pilchardus* in the Bay of Biscay. *Frontiers in Marine Science*, *7*. https://doi.org/10.3389/fmars.2020.567841

Violle, C., Navas, M.L., Vile, D., Kazakou, E., Fortunel, C., Hummel, I., and Garnier, E. (2007). Let the concept of trait be functional! Oikos, 116(5), 882-892. https://doi.org/10.1111/j.0030-1299.2007.15559.x

Watanabe, A. (2018). How many landmarks are enough to characterize shape and size variations? PLOS ONE, 13(6), e0198341.web

Webb, T.J., Vanden Berghe, E., and O'Dor, R. (2010). Biodiversity's big wet secret: the global distribution of mbarine biological records reveals chronic under-exploration of the deep pelagic ocean. PLoS ONE, 5(8), e10223. https://doi.org/10.1371/journal.pone.0010223

Widder, E.A. (2010). Bioluminescence in the ocean: origins of biological, chemical, and ecological diversity. Science, 328(5979), 704-708. https://doi.org/doi:10.1126/science.1174269